Initiated Chemical Vapor Deposition of Functional Polyacrylic Thin Films

by

Yu Mao

M.S. in Materials Science and Engineering
Massachusetts Institute of Technology, 2003

B.S. in Polymer Materials Science
Tsinghua University, 1998

Submitted to the Department of Materials Science and Engineering
in Partial Fulfillment of the Requirements for the Degree of

DOCTOR OF PHILOSOPHY IN MATERIALS SCIENCE AND ENGINEERING
AT THE
MASSACHUSETTS INSTITUTE OF TECHNOLOGY

September 2005

Signature of Author .....
Department of Materials Science and Engineering
May 18, 2005

Certified by .....
Karen K. Gleason
Professor of Chemical Engineering
Thesis Advisor

Certified by .....
Adam C. Powell IV
Professor of Materials Science and Engineering
Thesis Co-Advisor

Accepted by .....
Gerbrand Ceder
Professor of Materials Science and Engineering
Chairman, Departmental Committee on Graduate Students

Initiated Chemical Vapor Deposition of Functional Polyacrylic Thin Films

By

Yu Mao

Submitted to the Department of Materials Science and Engineering
on May 18, 2005 in Partial Fulfillment of the
Requirements for the Degree of
Doctor of Philosophy in Materials Science and Engineering

ABSTRACT

Initiated chemical vapor deposition (iCVD) was explored as a novel method for synthesis of functional polyacrylic thin films. The process introduces a peroxide initiator, which can be decomposed at low temperatures (<200°C) and initialize addition reaction of monomer species. The use of low temperatures limits the decomposition chemistry to the bond scission of initiator, while retaining functional groups of monomers, which has been confirmed in the infrared spectroscopy, nuclear magnetic resonance, and x-ray photoelectron spectroscopy of iCVD poly(glycidyl methacrylate) (PGMA) thin films. Studies of PGMA iCVD deposition kinetics and molecular weights indicate a free radical polymerization mechanism and provide guide for vapor-phase synthesis of other vinyl monomers. The retained epoxy groups can crosslink under e-beam irradiation, resulting in e-beam patterning of iCVD PGMA thin films with 80 nm negative-tone features achieved. iCVD copolymerization was also investigated to further tune film composition and properties. A surface propagation mechanism was proposed based on the study of the monomer reactivity ratios and the copolymer molecular weights during iCVD copolymerization. The synthesized acrylic copolymers have been investigated in applications as positive-tone e-beam resists, CO_2-developable resists, and low surface energy coatings with improved mechanical properties. The process of iCVD polymerization is extendable to vapor-phase polymerization of other vinyl monomers and creates new opportunities for the application of functional polymer thin films.

Thesis Supervisor: Karen K. Gleason
Title: Professor of Chemical Engineering

To My Family

Acknowledgements

I would like to express my gratitude to all those who provided the support and guidance throughout my thesis research.

I am indebted to my advisor, Karen, for being a tremendous support for this exciting research. Her enthusiasm, inspiration, and encouragement helped me in all the stages of my thesis research. Her guidance has made such a difference in my life and will continue to be my source of inspiration for pursuing my career.

My thesis committee members, Professor Samuel Allen, Professor Christine Ortiz, and Professor Adam Powell, provided insightful comments and suggestions on this research. Their inputs are highly appreciated. I am also very grateful for the advice of Professor Jian Yu about pursuing graduate study.

I would like to thank members of the Gleason group, past and present, for providing a supportive and enjoyable environment for my research. Their help and contributions have made my work such a wonderful experience. I'd like to especially thank Ken, Leslie, and Kelvin for generously sharing their expertise and offering their insights.

Thanks to all my friends whose friendship continues and sustains me. Special thanks go to Jin, Joy, and Yun, for your help and blessings during my difficult times; to Hanghui and Min, for being a source of guidance in my life and in my work; to Xiaohan, Mingyan, and Tao, for making my life so enjoyable.

Finally, I would like to express my deep gratitude to my family. To my parents, for opening the door to the outer world for me and implanting the spirit of exploration into my heart. To my sister, for always being supportive to my studies. To my husband, Tieming, for all the time we can talk, dream, exchange ideas, and share joy and frustrations together. This thesis could not have been accomplished without his support. The love and support from my family is my never-failing source of strength and inspiration.

TABLE OF CONTENTS

List of Figures

CHAPTER ONE

CHAPTER TWO

CHAPTER THREE

CHAPTER FOUR

CHAPTER FIVE

CHAPTER SIX

List of Tables

List of Acronyms, Abbreviations, and Symbols

AFM	Atomic Force Microscope
CVD	Chemical Vapor Deposition
E	Elastic Modulus
ESH	Environment, Safety and Health
f_A	mole fraction of monomer A
FTIR	Fourier Transform Infrared Spectroscopy
GPC	Gel Permeation Chromatography
H	Hardness
HFCVD	Hot Filament Chemical Vapor Deposition
iCVD	Initiated Chemical Vapor Deposition
MSE	Mean Squared Error
MAA	Methacrylic Acid
MCA	Methyl α-Chloroacrylate
M_n	Number-averaged Molecular Weight
M_w	Weight-averaged Molecular Weight
^{1}H NMR	Proton Nuclear Magnetic Resonance
PDI	Polydispersity Index
PECVD	Plasma-Enhanced Chemical Vapor Deposition
PGMA	Poly(glycidyl methacrylate)
PMMA	Poly(methyl methacrylate)
PPECVD	Pulsed Plasma-Enhanced Chemical Vapor Deposition
psi	Pound per Square Inch
PTFE	Poly(tetrafluoroethylene)
$P_{A,0}$	Equilibrium Pressure of Monomer A
r_A	Reactivity Ratio of Monomer A
RF	Radio Frequency
sc	Supercritical
sccm	Standard Cubic Centimeters per Minute
SEM	Scanning Electron Microscopy
T	Temperature
THF	Tetrahydrofuran
UV	Ultraviolet
VASE	Variable Angle Spectroscopic Ellipsometry
XPS	X-ray Photoelectron Spectroscopy
θ	Contact Angle
θ_{ad}	Advancing Contact Angle

CHAPTER ONE

Introduction

1.1 Chemical Vapor Deposition

In recent years we have witnessed increasing applications of functional polymer thin films in biotechnology and electronics. The need to improve devices' performance brings the inevitable requirement of producing high-quality surfaces and interfaces. Chemical vapor deposition (CVD) is a vacuum process that combines polymerization and coating into one single step. It provides surface coverage uniformity, small roughness, conformal coatings, and control over film composition, structure, and surface chemistry. It is capable of producing thin films on plastic substrates and complex substrates. In addition, it can be used to coat nanoscale features, as there are no surface tension and non-uniform wetting effects typically associated with wet processes.

Traditionally, CVD deposition is used to produce inorganic materials, such as those used in microelectronics fabrications. For organic functional thin film deposition, it is important to understand the method reactive species are activated and the way film growth proceeds. New processes and chemistry may also need to be designed and incorporated.

Plasma Enhanced Chemical Vapor Deposition (PECVD)

PECVD uses excitation of plasma to break down a precursor into many products such as neutral radicals, ions, and electrons. Neutral radicals are relatively benign species and diffuse to the substrate where they adsorb and polymerize on the surface, while ions are highly energized as a result of acceleration by the electric field: they collide with the substrate more forcibly and contribute to film damage and etching.[1] The plasma is induced using radio frequency (RF) power with high energy input (50-400W). Most often there is ultraviolet (UV) irradiation accompanied with the process.

Hot Filament Chemical Vapor Deposition (HFCVD)

HFCVD is a much "gentler" process compared with PECVD. In the HFCVD process, precursors are broken down by thermal decomposition. This setup employs resistively heated wires positioned in an array above the substrate to provide thermal energy. Generally HFCVD does not result in nonselective monomer fragmentation to the extent that PECVD does. Instead, precursors are decomposed into a fairly consistent group of polymerizable radicals, resulting in more controlled reaction pathways.

No electrons, ions, and UV irradiation are produced during HFCVD. The absence of ion bombardment and UV irradiation can minimize the amount of dangling bonds, which are commonly observed in PECVD films. In fact, HFCVD has been demonstrated as a method to synthesize fluorocarbon and siloxane films with much better-defined chemical structure than their corresponding PECVD films.[2]

Initiated Chemical Vapor Deposition (iCVD)

iCVD is a subset of HFCVD. This process introduces an initiator species into HFCVD, and it was first demonstrated for poly(tetrafluoroethylene) (PTFE) film deposition using a sulfonyl fluoride initiator.[3] The difference between iCVD and HFCVD is that decomposition of initiators generates radicals during iCVD, which subsequently react with monomers. The polymerization scheme is shown in Figure 1-1. The use of initiator in small concentrations resulted in enhanced deposition rates, more efficient utilization of precursor, and increased control over film composition and morphology.

More importantly, the iCVD PTFE film growth mechanism involves steps of initiation and propagation, which are similar to classical solution polymerization. The research about iCVD process suggests that other techniques relevant to classical polymer chemistry may be applied in the vacuum process of CVD. New opportunities may be created for the deposition of functional thin films by incorporating ideas used in solution polymerization into iCVD process. Of course, many questions are unanswered in this field. The most obvious question is the gap between the decomposition temperature of sulfonyl fluoride initiator (460°C) and the temperature that organic functional groups can be retained (< 300°C). Thus it is the intent of this thesis research to address some of these questions and provide insights for vapor phase synthesis of functional thin films.

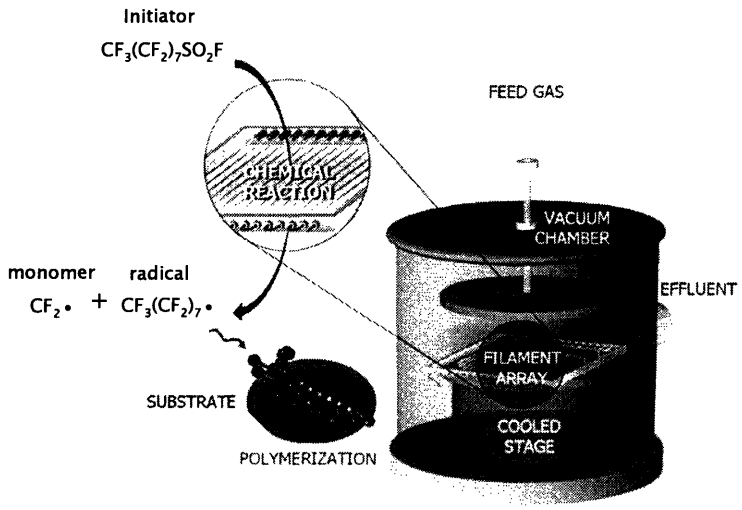

Figure 1-1. Schematic of iCVD process for PTFE thin film deposition using a sulfonyl fluoride initiator.

1.2 Solventless Lithography

Innovations in lithography have been central to advances in microelectronics fabrication. Conventional lithography uses an irradiation-sensitive material called resist to

transfer a pattern of radiation. As illustrated in Figure 1-2, the resist is first spun onto a silicon wafer, and then exposed to a source of photons or electrons through a mask that allows the irradiation to pass through a defined pattern. The exposed resist undergoes a chemical change (chain scission, crosslinking, or polarity change) and can either be selectively removed (positive tone) or remain (negative tone) on the wafer after development.[4]

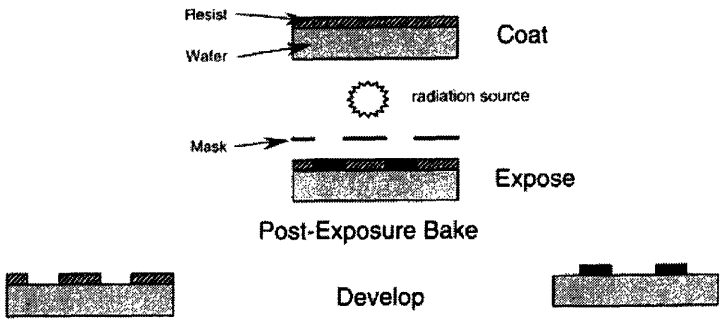

Figure 1-2. Process of conventional lithography.[4]

As high-speed electronic devices underwent dramatic changes over the past decade, increasing demands have been placed on lithography to further reduce feature size. At the same time, the semiconductor industry calls for continuing reduction of environmental, safety, and health (ESH) risks and costs associated with lithography. The solvent-intensive methodology in conventional lithography thus suffers from several disadvantages. First, only 2-5% of resist remains on the wafer after spin coating; more than 95% of material becomes waste and needs to be disposed safely.[5] Second, the significant amount of liquid solvents used in both spin-on and development processes pose risks for the environment and lead to potential hazard for the safety and health of workers. The costly disposal of solvents is not financially favorable to the industry. Furthermore, both organic and aqueous solvents have met the problem of pattern collapse in the development of high aspect ratio features.

The strategy is to design a solventless lithography process that completely eliminates the undesirable wet chemistry through incorporation of new processes and materials. The solution is to replace the "wet" spin-on process in thin film fabrication with a "dry" CVD method and to substitute the traditional "wet" development with a supercritical (sc) CO_2 process. Moving towards solventless lithography is advantageous since this "dry" processing requires less materials usage, fewer processing steps, lower energy consumption and waste disposal, translating to lower fabrication cost. The scheme of the solventless lithography with a positive tone is illustrated in Figure 1-3. Irradiation-sensitive films deposited using CVD are selectively irradiated, then films with the latent pattern are developed in a $scCO_2$ medium.

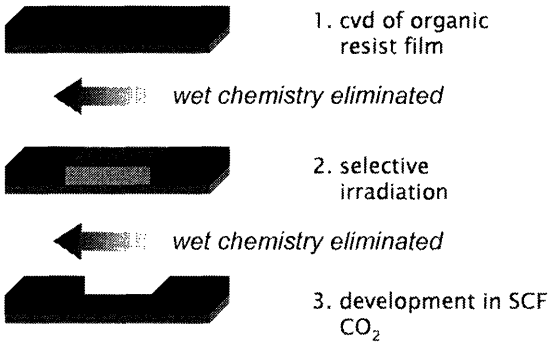

Figure 1-3. Schematic of solventless lithography.

For the microelectronics industry, CVD is believed to incur fewer penalties with respect to the environment, safety, and health.[5] Being an enclosed process, CVD raises no issues of exposure to solvents or volatile organic compounds. There are also no wastes or costs associated with solvents and rinse water that is inherent in a spin-on process. CVD resists are generally less complex than conventional resists, and thus less subject to degradations over time. Performance benefits may also accrue from the adoption of CVD

resists. CVD resist deposition is more compatible with other processes currently used in microfabrication.[1] The vacuum process of CVD allows production of cleaner surfaces with extremely small roughness. The conformal nature of the CVD process would enable patterning on non-planar substrates.[6] The vapor phase processing method is capable of fabricating thin films on soluble substrates and thus can be extended to a wider range of new material applications, such as patterning of organic electronics on plastics.[7]

However, the research of CVD resists is still being developed, and there is only a limited amount of literature in this area (Table 1-1) due to the difficulty to retain the delicate chemistry of resists using conventional CVD methods. To address this challenge, iCVD may be a viable process due to its selective reaction pathway, but initiator chemistry that can decompose at temperatures lower than the temperatures functional groups degrade needs to be explored.

Table 1-1. CVD resists

Materials	Exposure	Contrast	Sensitivity	Resolution	Reference
Plasma PMMA	e-beam	positive-tone	160 $\mu C/cm^2$	1 μm	Morita, 1980. Kim, 1999.
Plasma Organosilicon	UV 193 nm	negative-tone	20 mJ/cm^2	0.16 μm	Horn, 1990. Nalamasu,1997.

$scCO_2$ is envisioned as an "environmentally responsible" solvent and is widely used in food and pharmaceutical industries. $scCO_2$ technology has also gained considerable attention in the area of microelectronics, because $scCO_2$ possesses unique properties beneficial for development of small, high-aspect ratio features: low surface tension to prevent pattern collapse, high diffusivities comparable to those of gases, liquid-like densities and solvating powers adjustable through adjusting pressure and temperature.[8] The primary

challenge in using $scCO_2$ for the development of resists arises from the fact that only fluoropolymers and silicon-containing polymers are CO_2-philic.[9] Therefore it is imperative to tailor the composition of regular resists to make them processable in CO_2.

A positive-tone contrast has been demonstrated in CVD fluorocarbon films using e-beam irradiation and $scCO_2$ development.[10] Complete development using $scCO_2$ was obtained under an e-beam dosage of 6000 $\mu C/cm^2$ (Figure 1-4). The high dosage required for development of fluorocarbon films suggests that an order-of-magnitude increase of sensitivity is desired, since the dosage range for common e-beam resists is 10-100 $\mu C/cm^2$. Incorporation of functionalities that are more sensitive to e-beam irradiation would be necessary for the research of CVD resists.

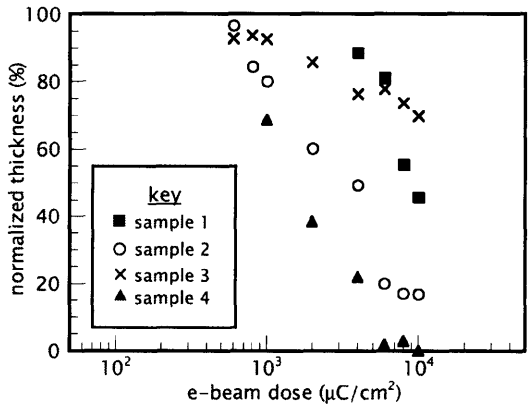

Figure 1-4. Contrast curves of CVD PTFE films.[10]

1.3 Low Surface Energy Coatings

Low surface energy finishes are desirable in many applications such as non-wettable and anti-fouling coatings for clothing, biomedical, and aerospace applications. Fluoropolymers such as poly(tetrafluoroethylene) (PTFE) (surface energy $\gamma_s \sim 20$ mN/m) and

fluorinated polyacrylics (γ_s < 10 mN/m) are widely used in creating low surface energy coatings.

However, difficulty exists for fabrication of both PTFE and fluorinated polyacrylic thin films. PTFE is poorly soluble in common solvents and thus cannot be formulated like traditional soluble resins. It must be applied as a dispersion of polymer particles and subsequently sintered at >350°C to form a film.[11] Fluorinated acrylic polymers demonstrate higher solubility than PTFE, but they still require partially fluorinated or other special solvents to cast a film. These harsh coating conditions limit the application of fluoropolymer thin films and call for the development of novel fabrication processes.

In addition, because the weak intermolecular forces between fluorinated chains limit the cohesion in the coatings, the mechanical properties of these fluoropolymer coatings are poor. For example, the hardness of PTFE (0.06 GPa)[12] is much lower than the hardness of most hydrocarbon polymers (~0.2 GPa).[13] The softness of coatings results in poor abrasion resistance. Thus, there is a clear need to modify the composition of fluoropolymer coatings to improve their mechanical properties.

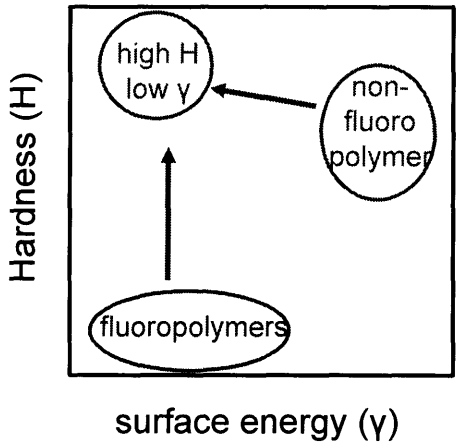

Figure 1-5. Design of thin films with low surface energy and high hardness.

The in-situ vapor phase synthesis of CVD can circumvent problems currently present in fabricating fluoropolymer thin films. CVD also provides tailoring of film composition for specific applications. Therefore it is promising to investigate CVD fluoropolymer coatings to optimize both mechanical and surface properties (Figure 1-5). Furthermore, because of the elimination of solvents and the conformal nature of coatings, CVD process is advantageous over traditional coating methods in its capability in retaining nanoscale features, which may create new opportunities to extend fluoropolymer coatings to nano technologies.

1.4 Scope of Thesis

Chapter 2 reports the iCVD of poly(glycidyl methacrylate) (PGMA) thin films. A new initiator, tert-butyl peroxide, was introduced into the iCVD process and allows film depositions at temperature <200°C. The complete retention of the pendant epoxy functionality was confirmed. This chapter explores the mechanism of the iCVD process and provides a guide for vapor phase synthesis of functional polymers.

Chapter 3 investigates the electron-beam patterning of the iCVD PGMA thin films with 80 nm negative-tone features achieved. Development of iCVD PGMA thin films in $scCO_2$ with co-solvents added indicates the potential for creating a solventless lithographic process.

Chapter 4 reports the first demonstration of iCVD copolymerization. Monomer reactivity ratios and propagation mechanism are investigated in detail and provide prediction of copolymer compositions. Copolymers of methyl α-chloroacrylate (MCA) and methacrylic

anhydride (MAH) were successfully synthesized using iCVD, and the post-annealed copolymer thin films achieved 60 nm positive-tone patterns using electron-beam irradiation.

Chapter 5 reports using iCVD copolymerization to incorporate fluorinated acrylics into irradiation-sensitive CVD thin films. Patterns were created in these iCVD copolymer thin films using e-beam irradiation and pure $scCO_2$ development, a complete solventless lithographic process.

Chapter 6 reports an iCVD copolymerization approach for the synthesis of low-surface-energy fluorinated coatings that can self-crosslink to achieve mechanical and optical properties superior to traditional hydrophobic polymer coatings.

Chapter 7 gives an overview of the progress made in iCVD synthesis of functional polyacrylic thin films and provides comments on possible future research directions stemming from results obtained in this thesis research.

Each chapter begins with the motivation and literature survey for each specific topic. Each chapter is formatted as a technical journal paper with experimental methods, results, discussions, and conclusions, so it can be read as an individual entity without referring to other chapters. Therefore, this present chapter only provides general background for the whole thesis.

1.5 References

(1) Lau, K. K. S. PhD Thesis. Massachusetts Institute of Technology, 2000.
(2) Lewis, H. G. P.; Edell, D. J.; Gleason, K. K. *Chem. Mat.* **2000,** *12*, 3488.
(3) Lewis, H. G. P.; Caulfield, J. A.; Gleason, K. K. *Langmuir* **2001,** *17*, 7652.

(4) Sundararajan, N.; Yang, S.; Ogino, K.; Valiyaveettil, S.; Wang, J. G.; Zhou, X. Y.; Ober, C. K.; Obendorf, S. K.; Allen, R. D. *Chem. Mat.* **2000,** *12*, 41.

(5) Labelle, C. B.; Gleason, K. K. *Abstr. Pap. Am. Chem. Soc.* **1998,** *216*, U81.

(6) Jeon, N. L.; Nuzzo, R. G.; Xia, Y. N.; Mrksich, M.; Whitesides, G. M. *Langmuir* **1995,** *11*, 3024.

(7) Forrest, S. R. *Nature* **2004,** *428*, 911.

(8) Weibel, G. L.; Ober, C. K. *Microelectron. Eng.* **2003,** *65*, 145.

(9) McHugh, M. A.; Krukonis, V. J. *Supercritical Fluids Extraction: Principles and Practice*. 2nd ed.; Butterworth-Heineman: Stoneham, MA, 1993.

(10) Lewis, H. G. P.; Weibel, G. L.; Ober, C. K.; Gleason, K. K. *Chem. Vapor Depos.* **2001,** *7*, 195.

(11) Anton, D. *Adv. Mater.* **1998,** *10*, 1197.

(12) Wang, J.; Shi, F. G.; Nieh, T. G.; Zhao, B.; Brongo, M. R.; Qu, S.; Rosenmayer, T. *Scr. Mater.* **2000,** *42*, 687.

(13) Briscoe, B. J.; Fiori, L.; Pelillo, E. *J. Phys. D-Appl. Phys.* **1998,** *31*, 2395.

CHAPTER TWO

Hot Filament Chemical Vapor Deposition of Poly(glycidyl methacrylate) Thin Films Using Tert-butyl Peroxide as an Initiator

Y. Mao and K. K. Gleason, *Langmuir* **20**, 2484 (2004).

Abstract

We have demonstrated the successful deposition of poly(glycidyl methacrylate) (PGMA) thin films using hot filament chemical vapor deposition (HFCVD) with tert-butyl peroxide as the initiator. The introduction of the initiator allows film depositions at low filament temperature (<200°C) and greatly improves film deposition rates. The retention of the pendant epoxide chemical functionality and the linear polymeric structure in the deposited films were confirmed by infrared spectroscopy and X-ray photoelectron spectroscopy. The number-average molecular weight of PGMA films can be systematically varied from 16,000 to 33,000 by adjusting the filament temperature and the flow ratio of initiator to precursor. The apparent activation energies observed from PGMA deposition kinetics (100.9±9.6 kJ/mol) and from molecular weight measurement (-54.8±2.0 kJ/mol) are close to the calculated overall activation energies for polymerization rate (104.4 kJ/mol) and for number-average molecular weight (-59.2 kJ/mol), which supports the hypothesis of free radical polymerization mechanism in the HFCVD PGMA deposition.

Acknowledgements

We gratefully acknowledge the support of the NSF/SRC Engineering Research Center for Environmentally Benign Semiconductor Manufacturing. This work also made use of MRSEC Shared Facilities supported by the National Science Foundation under Award Number DMR-9400334. We also thank Professor Paula T. Hammond's group at MIT for help with GPC experiments.

2.1 Introduction

Glycidyl methacrylate (GMA) is a desirable chemically reactive species because its epoxy group could be converted into different kinds of functionalities through ring-opening reaction. This reaction provides various opportunities for applications in polymer surface modification,[1] high-performance membrane[2] and resist imaging.[3,4] In particular, the crosslinking reaction of the epoxy group in poly (glycidyl methacrylate) (PGMA) under electron-beam exposure creates the potential for a high-sensitivity negative tone electron-beam resist.[5] A sensitivity of 0.5 $\mu C/cm^2$ was reported for spin-coated PGMA under electron-beam acceleration voltage of 5-10 kV.[3]

Typically, PGMA is polymerized in the solution phase and thin films are deposited by spin casting.[3] Alternatively, vapor phase deposition of thin films from plasma excitation of GMA has been investigated for PTFE surface modification or for polyimide adhesion promotion.[6,7] By controlling plasma deposition conditions, the epoxide functional groups could be preserved to various extents.

In this paper, the hot filament chemical vapor deposition (HFCVD) of PGMA is demonstrated as a route for retaining epoxide functionalities in the deposited films. The low excitation energies of HFCVD process also allow for achieving linear polymeric structure and designing film stoichiometry through control over precursor polymerization pathways. HFCVD has been used to produce linear polyoxymethylene chains,[8] polymeric fluorocarbon films spectroscopically similar to poly(tetrafluoroethylene),[9] and organosilicon films that consist of linear and cyclic siloxane repeat units.[10] Recently it was found that the introduction of initiator species in HFCVD provides greater control over both chemical compositions and growth rates for fluorocarbon and organosilicon films.[11,12] Vapor phase deposition is

advantageous over solution phase deposition such as spin casting, because it is capable of coating thin films on substrates with complex geometries.[13] The process of vapor phase deposition is relatively simple and has more flexibility for integration with other processes. Moreover, vapor phase deposition does not involve use of solvents and has less impact on environment.

This paper reports the deposition of PGMA films through HFCVD from precursor GMA. The effect of adding a new initiator species, tert-butyl peroxide, to the HFCVD process will be discussed. The retention of irradiation-sensitive group and the linear polymeric structure, which are achieved through this novel process, create new opportunities for PGMA thin films applications.

2.2 Experimental Methods

Films were deposited on silicon wafer substrates in a home-built reactor. In the HFCVD process, thermal excitation was provided by resistively heating up a Nichrome filament (80% Ni/20% Cr) mounted in a parallel array. The filament holder was straddled on a stage maintained at 25°C using water cooling. The distance between the filament and the stage was 2.2 cm. Pressure in the vacuum chamber was maintained at 0.5 torr using a butterfly valve. In the plasma enhanced chemical vapor deposition (PECVD) system, a low radiofrequency power of 10 W was applied continuously between the upper electrode and the grounded lower electrode. The pressure in the PECVD system was kept at 0.2 torr.

GMA precursor (Aldrich) was vaporized in a glass jar which was heated up to 65±3°C and fed into the reactor through a line maintained at 90±5°C. Tert-butyl peroxide (Aldrich) was vaporized in a glass container at room temperature and fed through a different port. The

precursor and the initiator are mixed together after entering into the reactor. The flow rate of both GMA and tert-butyl peroxide were regulated using needle valves. To evaluate the effect of initiator/precursor flow ratio on the deposition rate, GMA flow rate was kept constant at 3 sccm, while the flow rate of tert-butyl peroxide was varied between 0 and 2.5 sccm. Films were deposited at filament temperature of 180°C-250°C. Filament temperature was measured using a thermocouple directly attached to one of the filaments. Depositions were monitored by reflectance on silicon substrates using interferometry with a He-Ne 632.8 nm laser light. Cycle thickness was calculated using the wavelength, the incidence angle (24°) and the refractive index of PGMA film (1.50), and it corresponded well with the data obtained from variable angle spectroscopic ellipsometry (VASE). Details about VASE have been described previously.[14]

Fourier transform infrared (FTIR) measurements were done on a Nicolet Nexus 870 spectrometer in normal transmission mode using a DTGS KBr detector over the range of 400-4000 cm^{-1} at 4 cm^{-1} resolution. Films deposited by CVD were measured under FTIR immediately after the deposition. Conventionally-polymerized PGMA was obtained from Polymer Source (Canada) and dissolved in acetone to form a 10-15 wt% solution. The solution was spun on a silicon wafer to form a film with thickness of ~300 nm for FTIR measurements. X-ray photoelectron spectroscopy (XPS) was carried out on a Kratos Axis Ultra spectrometer using a monochromatized aluminum K α source. Optical microscopy was done on Olympus CX41 microscope with eyepiece magnification of 10X and objective magnification of 100X. Film molecular weight was measured using Gel Permeation Chromatography (GPC) with a Waters 1525 Binary HPLC pump equipped with three columns from Waters Corp. A Waters R410 differential refractometer was used as the

detector. Polystyrene standards (Aldrich) were used for calibration at 30°C, and tetrahydrogen furan (THF) was used as the eluent.

2.3 Results and Discussion

Deposition Kinetics. Deposition of PGMA films using HFCVD without the initiator could be achieved with filament temperature greater than 220°C. However, the deposition rate is relatively low (less than 10 nm/min). The addition of the initiator tert-butyl peroxide to the process increases the deposition rate significantly and permits deposition at a temperature lower than 220°C, as shown in Figure 2-1a. The deposition rate is observed to be low order in tert-butyl peroxide if the initiator/precursor flow ratio is above 0.32. Deposition rate increases as filament temperature increases from 185°C to 222°C. As filament temperature further increases, the deposition rate decreases. Using the highest deposition rate, 146 nm/min, the fraction of consumed GMA was calculated to be ~6% using the mass of the deposited film divided by the mass of GMA monomer flowing into the reactor. With this low conversion of GMA, the concentration of GMA in the reactor will be treated as a constant, allowing the overall kinetic expression to be simplified resulting in the measured deposition rate being proportionally related to the overall reaction rate constant. Thus deposition rate as a function of filament temperature could be plotted in Arrhenius form[11,13] in the temperature range of 185°C to 222°C, as indicated in Figure 2-1b. The average deposition rate for initiator/precursor flow ratio 0.32, 0.52, and 0.85 are used in Figure 2-1b with standard deviations indicated by error bars. An apparent activation energy of 100.9±9.6 kJ/mol is calculated from the slope of the least squares linear regression to the data. It is postulated that the film growth is limited by initiation in the filament temperature range of 185°C-222°C

since PGMA cannot be deposited without the initiator in this temperature range. The decrease in deposition rate above filament temperature 222°C is attributed to onset of gas-phase reaction resulting in the observed coarse film morphology.[13]

Film Structure. Figure 2-2 shows the FTIR spectrum of a PGMA film synthesized from HFCVD, compared with the spectra of conventionally-polymerized PGMA and a film deposited from PECVD of GMA. The HFCVD film was grown under filament temperature 222°C with pressure 0.5 torr, GMA flow rate of 2.0 sccm and tert-butyl peroxide flow rate of 0.34 sccm. The PECVD film was deposited under continuous plasma power of 10 W with pressure 0.2 torr and GMA flow rate of 2.0 sccm. The growth rate for this PECVD GMA film was 35 nm/min. The FTIR bands in the PGMA film deposited from HFCVD are narrow and could be distinctly resolved, demonstrating specific chemical bonds only present in linear PGMA. Especially, the adsorption peaks at 907 cm^{-1}, 848 cm^{-1} and 760 cm^{-1} assigned to characteristic epoxide group adsorption bands from literature[1,15,16] are all displayed in the FTIR spectrum of the HFCVD film. In contrast, the peak broadening and the peak intensity loss in the spectrum of the plasma deposited film reflect large distribution of chemical bonding and destruction of functional groups, including the pendant epoxide group of GMA.

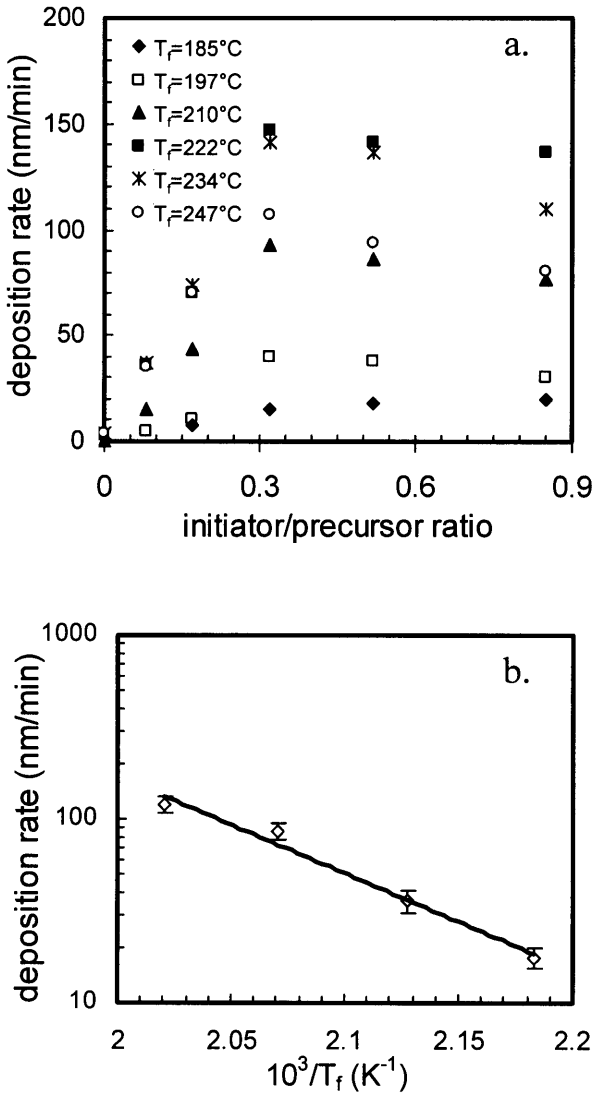

Figure 2-1. Deposition rate of PGMA films (a) as a function of increasing the tert-butyl peroxide flow rate in order to observe the effect of increasing the initiator/precursor flow ratio and (b) as a function of filament temperature plotted in Arrhenius form. The average deposition rate for initiator/precursor ratio 0.32, 0.52, and 0.85 are used in panel b with standard deviations indicated by error bars. An apparent activation energy of 100.9 ± 9.6 kJ/mol is calculated from the slope of the least squares linear regression to the data.

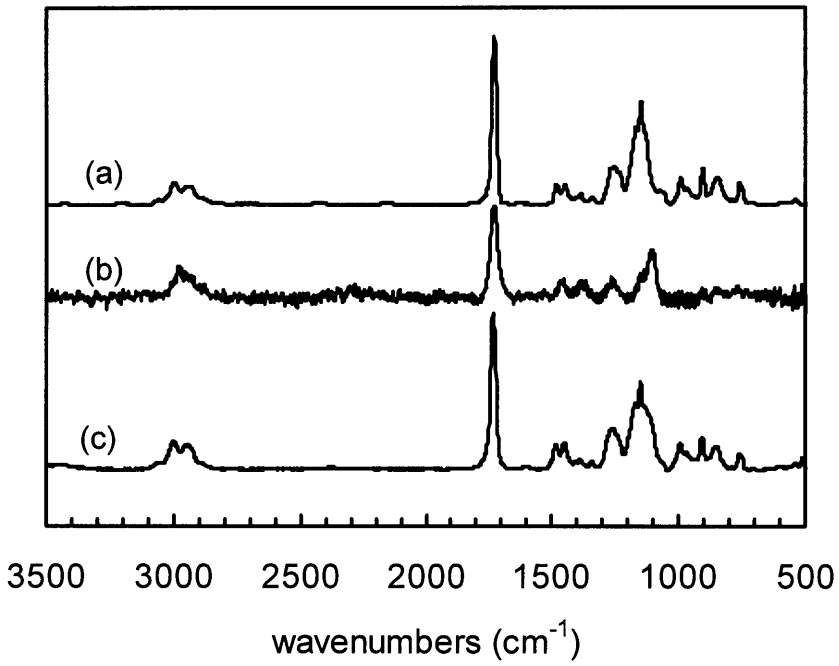

Figure 2-2. FTIR spectra of (a) PGMA film synthesized from HFCVD, (b) film deposited from low-power PECVD of GMA, and (c) conventionally-polymerized PGMA. The adsorption peaks at 907, 848, and 760 cm^{-1} are assigned to the characteristic adsorption bands of epoxide group.

The C 1s and O 1s high-resolution XPS scans for PGMA film synthesized from HFCVD (Figure 2-3) indicate five different types of carbon moieties and three different types of oxygen moieties. The fitted curves reproduce the observed spectra very well. Table 2-1 shows excellent agreement of both the binding energies and peak area ratios of the HFCVD film with previously reported results for solution polymerized PGMA.[17] The fittings were performed by fixing peak widths to the same values reported for solution polymerized PGMA and fixing the Gaussian/Lorentzian mixing ratio to 70/30.

The remarkable similarity of the XPS and FTIR spectra from both materials supports the hypothesis that the HFCVD 1) produces the same linear polymeric structure as

conventionally-polymerized PGMA and 2) retains essentially all of the pendant epoxide functional groups.

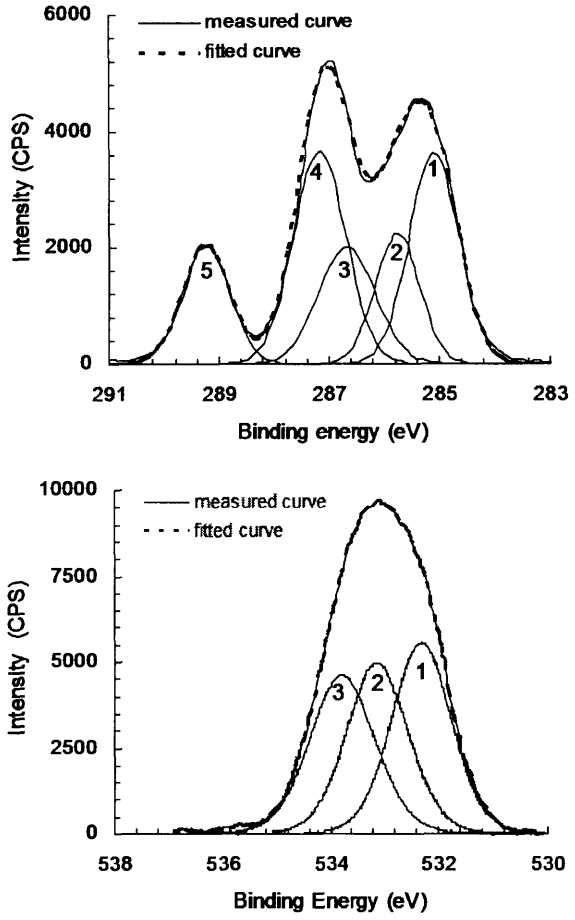

Figure 2-3. C 1s and O 1s high-resolution XPS scans of PGMA film deposited from HFCVD. The excellent agreement of both the binding energies and peak area ratios of the HFCVD film with reported results for solution-polymerized PGMA (Table 2-1) strongly supports the linear polymer structure and retention of pendant epoxide rings in the HFCVD films.

Film Morphology. The PGMA films deposited from HFCVD were investigated under optical microscopy. Most of the films are very smooth and featureless except for deposits using a very low initiator/precursor flow ratio 0.08. The morphologies resulting under the

condition of this low initiator flow rate are shown by a series of optical micrographs (Figure 2-4). The four films have approximately the same thickness (~300 nm). The film deposited at filament temperature 185°C shows a worm-like morphology which has been observed in other thin films grow by HFCVD.[18] It is postulated that film growth is dominated by initiation in this filament temperature range. The large feature size of around 10 μm results because only a small fraction of initiator was activated at this low temperature, resulting in limited density of nucleation sites formed on the surface. Once nucleated, the feature is able to rapidly grow to a large size. As filament temperature increases to 210°C and 222°C, film morphology is observed to be smoother with much smaller features. The change in film morphology was attributed to the increase of initiation and nucleation with increasing filament temperature. PGMA films deposited at a filament temperature of 247°C shows a granular morphology with particle size in the range of 2-3 μm. This coarse morphology was attributed to the domination of gas-phase reaction when filament temperature is high enough in the HFCVD process.[13]

Table 2-1. High-resolution XPS scan data of PGMA film deposited from HFCVD

			HFCVD PGMA film		PGMA reference[17]	
core level	peak	origin	binding energy (eV)	area (%)	binding energy (eV)	area (%)
C 1s	1	-C*H$_3$, -C-C*H$_2$-C-	284.96	29	285.00	29
	2	-C*(CH$_3$)-CO-	285.67	14	285.67	15
	3	-O-C*H$_2$-	286.68	16	286.71	15
	4	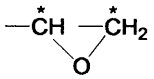	287.02	28	287.02	29
	5	-C*=O	289.15	13	289.15	13
O 1s	1	-C=O*	532.30	35	532.32	33
	2	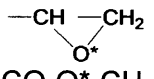	533.12	33	533.13	34
	3	-CO-O*-CH$_2$-	533.79	32	533.79	34

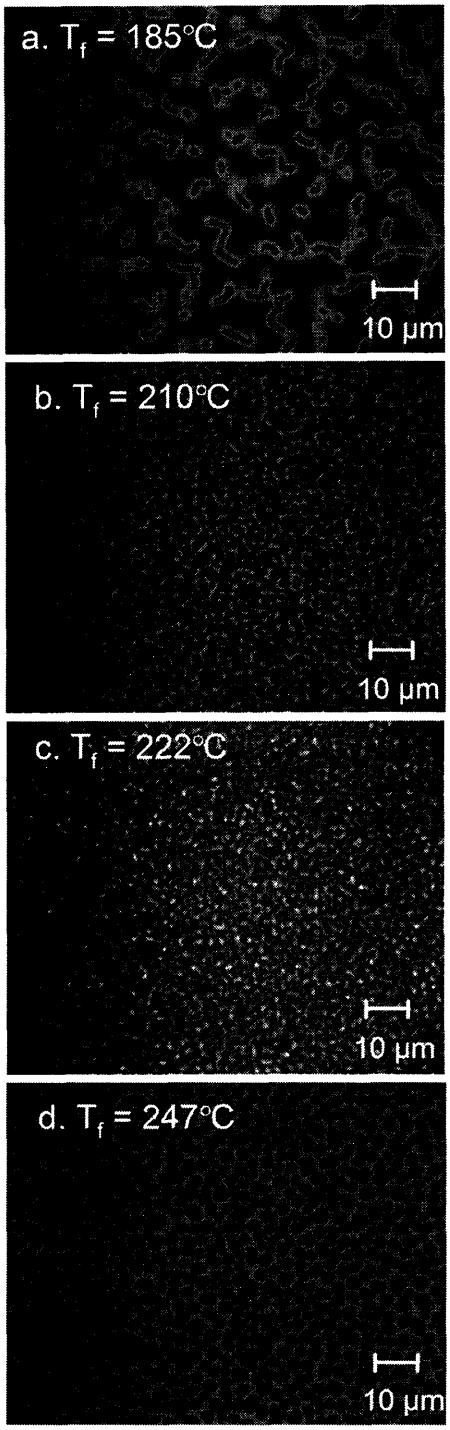

Figure 2-4. Optical micrographs showing effect of filament temperature on PGMA film morphology. PGMA films were deposited at (a) 185°C, (b) 210°C, (c) 222°C, and (d) 247°C using a low initiator/precursor flow ratio of 0.08. The thickness of these four films was approximately the same (~310 nm).

Molecular Weight. The ability to completely dissolve PGMA films deposited from HFCVD in solvent THF for GPC molecular weight analysis, confirms that the HFCVD process produces few if any crosslinks. By contrast, the PECVD GMA film was virtually insoluble under comparable conditions. Figure 2-5a shows the change of the PGMA film number-average molecular weight with HFCVD filament temperature. As filament temperature increases from 210°C to 234°C, the film molecular weight decreases rapidly. The number-average molecular weight as a function of the filament temperature could be plotted in a logarithmic form in this temperature range, as shown in Figure 2-5b. Using least squares linear regression to the data, the overall activation energy for the molecular weight could be computed from the slope of the regressed line. A value of -54.8 ± 2.0 kJ/mol is calculated. However, as filament temperature exceeds 234°C, the decrease of molecular weight is very small. For example, when the initiator/precursor flow ratio is 0.85, as filament temperature increases from 234°C to 247°C, the number-average molecular weight only decreases from 19,200 to 18,300. As filament temperature further increases, the curve of film number-average molecular weight reaches a plateau at around 16,000. Furthermore, even a great increase in initiator/precursor flow ratio has limiting effect in reducing film molecular weight.

The postulated onset of gas-phase reaction in HFCVD when the filament temperature is high enough or there is a supersaturation of reactive species[13] provides an explanation for the above results. The low-molecular-weight species generated in gas-phase reaction are difficult to precipitate and eventually pumped out of the reactor due to their low adsorption coefficient on the substrate. Thus, these low-molecular-weight fragments make no contribution to the overall molecular weight of deposited films.

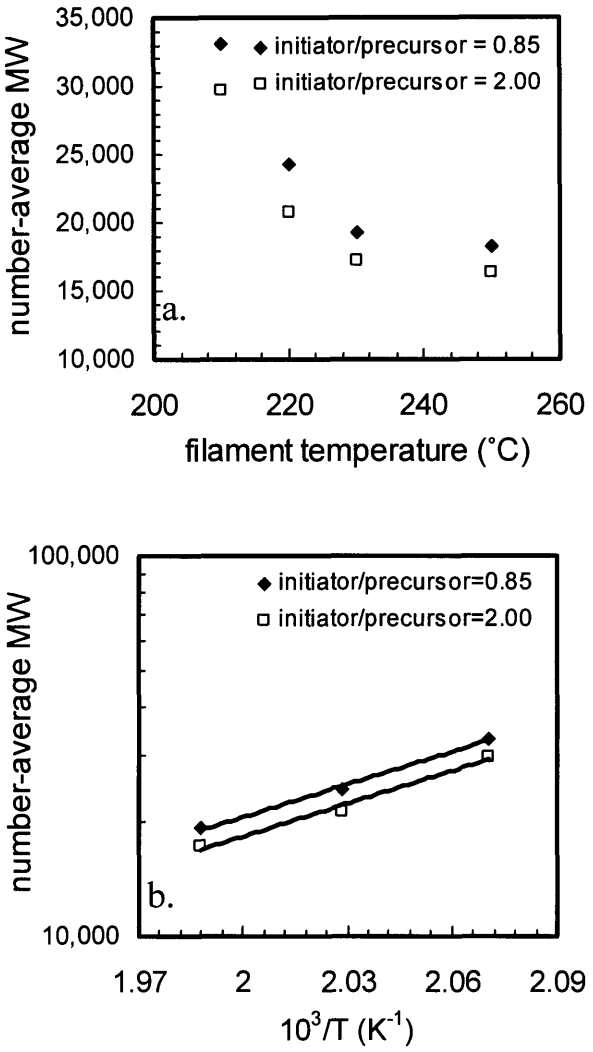

Figure 2-5. Number-average molecular weight of PGMA films (a) as a function of filament temperature and initiator/precursor flow ratio and (b) as a function of filament temperature plotted in logarithmic form. The overall activation energy for the molecular weight is computed to be -54.8 ± 2.0 kJ/mol using least squares linear regression to the data.

Reaction Chemistry. Tert-butyl peroxide is widely used as a free radical initiator in conventional polymerizations. The peroxide bond is easy to dissociate under low temperature (<150°C).[19] Similar thermal homolytic dissociation is expected to happen in the process of

HFCVD and generates tert-butyl radicals, as illustrated in Figure 2-6. The formation of tert-butyl radicals initializes the polymerization of GMA, similar to the steps in conventional polymerization. Termination can occur either through reaction of the propagating long-chain radical with the tert-butyl radical or through the coupling of two long-chain radicals.

The postulated polymerization mechanism provides an explanation for the deposition of PGMA films at lower filament temperatures and the higher film deposition rate with the introduction of a small amount of initiator. It is also consistent with the result of linear polymeric structure obtained in PGMA films deposited from HFCVD. The polydispersity index of HFCVD PGMA film molecular weight is in the range of 2.5-4.0, which is typical for free radical polymerization.[19]

Furthermore, the overall activation energy E_R of the polymerization rate for this polymerization scheme could be calculated as $[E_p + (E_d - E_t)/2]$,[19] where E_p, E_d and E_t are the activation energies of propagation, decomposition and termination respectively. E_d (163.6 kJ/mol) was obtained from reported data of tert-butyl peroxide decomposition in vapor phase, and E_p (22.6 kJ/mol) was estimated from the data of methyl methacrylate polymerization.[20] The value of E_t was estimated to be zero as radical termination reaction has nearly zero activation energy.[20] With these values, E_R is calculated to be 104.4 kJ/mol, which is very close to the value of the apparent activation energy (100.9 ± 9.6 kJ/mol) observed from the deposition kinetics (Figure 2-1). Similarly, the overall activation energy E_M of the number-average molecular weight can be calculated as $[E_p - (E_d + E_t)/2]$.[19] The result of this calculation, -59.2 kJ/mol, is a value close to the result (-54.8 ± 2.0 kJ/mol) obtained from molecular weight measurements of Figure 2-5. The close match of the results from our

experiments with the calculation results strongly supports the free radical reaction mechanism in the HFCVD process of PGMA films.

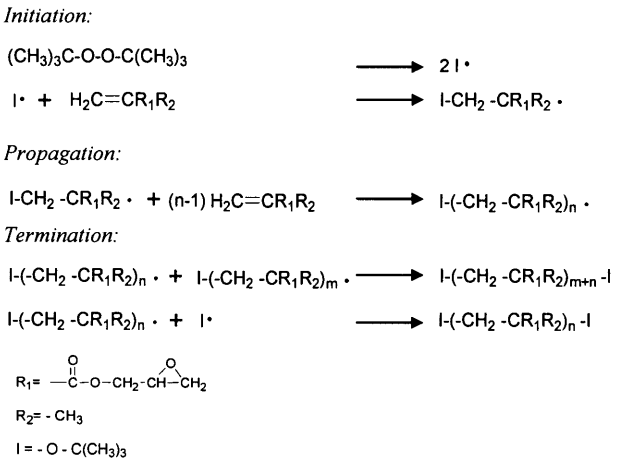

Figure 2-6. Postulated free radical reaction mechanism in PGMA film depositions using HFCVD with tert-butyl peroxide as an initiator.

2.4 Conclusions

PGMA thin films can be synthesized using HFCVD with GMA as the monomer. The introduction of tert-butyl peroxide as an initiator allows film deposition at low filament temperature (<200°C) and greatly improves the film deposition rate. The HFCVD method is advantageous over the conventional PECVD process in producing linear chemical structure and in retention of the pendant epoxide chemical functionality. The similarity of HFCVD PGMA films to the conventionally synthesized polymer was confirmed by FTIR and X-ray photoelectron spectroscopy. Molecular weight can be systematically varied by adjusting filament temperature and the flow ratio of initiator to precursor. The HFCVD process with tert-butyl peroxide as the initiator proceeds with a free radical reaction mechanism similar to classical free radical polymerization of vinyl monomers.

2.5 References

(1) Yang, G. H.; Kang, E. T.; Neoh, K. G. *J. Polym. Sci. Pol. Chem.* **2000**, *38*, 3498.

(2) Lee, W.; Oshikiri, T.; et al. *Chem. Mater.* **1996**, *8*, 2618.

(3) Thompson, L. F.; Feit, E. D.; et al. *Polym. Eng. Sci.* **1974**, *14*, 529.

(4) Shirai, M.;Sumino, T.; Tsunooka, M. *ACS Sym. Ser.* **1994**, 579, 185.

(5) Thompson, L. F.; Willson, C. G. *Introduction to Microlithography*, 2nd ed.; American Chemical Society: Washington, DC, 1994.

(6) Zou, X. P.; Kang, E. T.; Neoh, K. G.; et al. *Polym. Advan. Technol.* **2001**, *12*, 583.

(7) Yang, G. H.; Kang, E. T.; Neoh, K. G. *J. Adhes. Sci. and Technol.* **2001**, *15*, 727.

(8) Loo, L. S.; Gleason, K. K. *Electrochem. Solid St.* **2001**, *4*, G81.

(9) Lau, K. K. S.; Gleason, K. K. *J. Fluorine Chem.* **2000**, *104*, 119.

(10) Pryce Lewis, H. G.; Casserly, T. B.; Gleason, K. K. *J. Electrochem. Soc.* **2001**, *148*, F212.

(11) Pryce Lewis, H. G.; Caulfield, J. A.; Gleason, K. K. *Langmuir* **2001**, *17*, 7652.

(12) Murthy, S. K.; Olsen, B.; Gleason, K. K. *Langmuir* **2002**, *18*, 6424.

(13) Pierson, H. O. *Handbook of Chemical Vapor Deposition,* 2nd ed.; Noyes Publications: Norwich, NY, 1999.

(14) Lau, K. K. S.; Caulfield, J. A.; Gleason, K. K. *J. Vac. Sci. Technol. A.* **2000**, *18*, 2404.

(15) Davidson, K.; El-Attawy S.; El-Gamal M., et al. *High Perform. Polym.* **2002**, *14,* 3.

(16) Kumar, R. N.; Woo, C. K.; Abusamah, A. *J. Appl. Polym. Sci.* **1999**, *73*, 1569.

(17) Beamson, G.; Briggs, D. *High Resolution XPS of Organic Polymer*; John Wiley & Sons: Chichester, England, 1992.

(18) Hwang, N. M.; Cheong, W. S.; Yoon, Kim D.; et al. *J. Cryst. Growth* **2000**, *218*, 33.

(19) Odian, G. *Principles of Polymerization*, 2nd ed.;Wiley-Interscience: New York, 1981.

(20) Brandrup, J.; Immergut, E. H.; Grulke E. A. Editors. *Polymer Handbook*, 4th ed.; Wiley Interscience: New York, 1999, Section II, p 27 and p 419.

CHAPTER THREE

Electron-beam Patternable Poly(glycidyl methacrylate) Thin Films from Hot Filament Chemical Vapor Deposition

Y. Mao, N. M. Felix, P. T. Nguyen, C. K. Ober, and K. K. Gleason, *Journal of Vacuum Science and Technology B,* **22**, 2473 (2004).

Abstract

Chemical vapor deposition (CVD) of resist thin films is a dry processing alternative to the conventional spin casting of resists. However, the sensitivity and resolution of plasma CVD resists are limited due to the crosslinked structure in the deposited films. In this study, we demonstrated hot filament chemical vapor deposition (HFCVD) of poly(glycidyl methacrylate) (PGMA) thin films with improved sensitivity and resolution under electron-beam irradiation. We also demonstrated supercritical CO_2 development of the HFCVD PGMA thin films, which indicates the potential for an "all-dry" lithographic process. The pendent epoxide groups were retained in the low-energy HFCVD process, and linear polymeric structure was achieved. The HFCVD PGMA films have an electron-beam sensitivity of 27 $\mu C/cm^2$ using conventional development and an electron-beam sensitivity of 15 $\mu C/cm^2$ using supercritical CO_2 development. Decreasing film number-average molecular weight, M_n, decreases sensitivity but improves resolution by alleviating the swelling of small features. The PGMA film with M_n 4,700 g/mol resolved 80 nm features using conventional development and 300 nm features using supercritical CO_2 development.

Acknowledgements

We gratefully acknowledge the support of the NSF/SRC Engineering Research Center for Environmentally Benign Semiconductor Manufacturing. This work made use of MIT's shared scanning-electron-beam-lithography facility in the Research Laboratory of Electronics (SEBL at RLE), the Cornell Nanoscale Facility, MRSEC Shared Facilities supported by the National Science Foundation under Award Number DMR-9400334, and the NMR facilities of Chemistry Department at MIT. We also thank Professor Paula T. Hammond's group at MIT for help with GPC experiments.

3.1 Introduction

Increasing demands have been placed on lithography to further decrease feature size and improve resolution over the past decade.[1] At the same time, there has been an increasing awareness of environmental, safety and health (ESH) issues. Elimination of wet chemistry during the deposition and/or development steps reduces volatile organic compound emissions and alleviates ESH impacts of lithography. Several approaches have been tried to incorporate chemical vapor deposition (CVD) of resist thin films as part of a dry lithography process.[1-5] Using the vacuum process of CVD, there is potential for improving lithographic performance by achieving a cleaner surface. Unlike the solvent-based resins employed for spin-coating resists, CVD monomers are small molecules that can be purified to a high degree and have a long shelf life.[6] Furthermore, vapor phase deposition is relatively simple and has more flexibility for integration with other processes. The conformal nature of many CVD processes would also allow application of resist layers onto nonplanar substrates.

As another part of a dry lithography process, supercritical CO_2 has been demonstrated as a potential environmentally-benign replacement for organic development and cleaning solvents. At conditions above 31°C and 1070 psi, CO_2 exists in the supercritical state. Its synergistic properties—such as its lack of surface tension, its high density, and high diffusivity—prevent pattern collapse and enhance performance for development of high-aspect-ratio features.[7] Previous researchers have demonstrated the ability of supercritical CO_2 to dissolve many varieties of polymers.[8,9] In particular, fluorinated polymers and certain polysiloxanes have been found to be highly soluble in supercritical CO_2 under moderate conditions.[10,11] An alternative route to improve polymer solubility in supercritical CO_2 is the addition of a small amount of cosolvents to the supercritical fluid, which has been shown to

drastically increase the solvating power of the fluid[8,12] and provides the potential for supercritical CO_2 development of a wide range of resists.

Organosilicon thin films grown by plasma CVD have been explored as dry resists for 193 nm ultraviolet (UV) lithography.[3,5] Using a dosage of 20 mJ/cm^2, a 0.16 μm line pattern has been demonstrated for plasma polymerized methyl silane.[5] However, the research was not continued due to the instability of polysilane films caused by moisture adsorption. Additionally, the approach of patterning polysilane films can not be extended to 157 nm UV lithography, because the imaging process needs oxygen, which absorbs photons at 157 nm. Plasma polymerized methyl methacrylate was also explored as an electron-beam resist.[1] Crosslinked structures were formed in these films due to the plasma process, thus high dosage (160 μC/cm^2 at an acceleration voltage of 20 kV) was needed to achieve that contrast. Thus it is the intent of our research to produce uncrosslinked CVD thin films that are stable in the atmosphere and can be developed using supercritical CO_2.

Hot filament chemical vapor deposition (HFCVD) has been demonstrated as a route to achieve linear polymeric structure and control over film stoichiometry, because the selective excitation of chemical pathways in the process can avoid undesirable reactions, such as those leading to crosslinking and dangling bond defects. Polyoxymethylene,[13] polymeric fluorocarbon films[14] and polymeric organosilicon films[15] have been produced using HFCVD. In particular, the introduction of initiator species into the HFCVD process further lowers filament temperatures[16,17] and provides the potential to synthesize polymers with delicate functionalities. Recently, we have reported using initiated HFCVD to produce poly(glycidyl methacrylate) (PGMA) thin films. [18]

Previous research has shown a high sensitivity of ~0.5 $\mu C/cm^2$ for the conventionally-polymerized PGMA under an electron-beam acceleration voltage of 5-10 kV.[19,20] The copolymer of GMA and ethyl acrylate has served as ion milling and back sputtering mask.[19] In this paper, we examine the potential of using HFCVD deposited PGMA thin films for electron-beam resist applications. After conventional development was explored to investigate the lithographic performance of the HFCVD PGMA films, supercritical CO_2 was used for the development of HFCVD thin films.

3.2 Experiment

A. Film Preparation

Films were deposited onto silicon wafer substrates without any pretreatments in a home-built reactor which can accommodate silicon wafers up to 200 mm in diameter.[21] Thermal excitation was provided by resistively heating up stainless steel filaments (72%Fe/18%Cr/10%Ni) mounted in a parallel array to a temperature of 180°C-250°C. Filament temperature was measured using a thermocouple directly attached to one of the filaments. The filament holder was straddled on a stage maintained at 25°C using water cooling. The distance between the filament and the stage was 2.0 cm. Pressure in the vacuum chamber was maintained at 0.5 torr using a butterfly valve. Glycidyl methacrylate (GMA) precursor (Aldrich) was heated to 65±3°C and vaporized into the reactor through a line maintained at 90±5°C. Tert-butyl peroxide (Aldrich) was vaporized at room temperature and fed into the reactor through a different port. The flow rates of both GMA and tert-butyl peroxide were regulated using needle valves. The GMA flow rate was kept constant at 2

sccm, while the flow rate of tert-butyl peroxide was varied between 1 sccm and 2.4 sccm to obtain films with different molecular weights.

Solution-polymerized PGMA was obtained from Polymer Source (Canada) and dissolved in acetone to form a 10 wt% solution. The solution was filtered using 0.2 μm PTFE filters and spun onto a silicon wafer. The formed film was baked at 70 °C in a vacuum oven for 1 hr.

B. Film Characterization

Room temperature ^{1}H NMR spectra were taken at 300 MHz using a Varian Unity 300 spectrometer. The PGMA films were dissolved in deuterated chloroform ($CDCl_3$), and chemical shifts were determined by reference to the solvent peak. Atomic force microscopy (AFM) was performed on a Digital Instruments Dimension 3000 under tapping mode with a standard etched silicon tip. A blank silicon wafer was used for calibration. The image was accepted only when both the trace and retrace scans were visually identical. Film molecular weight was measured using Gel Permeation Chromatography (GPC) with a Waters 1525 Binary HPLC pump equipped with three columns from Waters Corp. Polystyrene standards (Aldrich) were used for calibration, and tetrahydrofuran was used as the eluent. Film thickness was measured using profilometry. Table 3-1 summarizes the characteristics of five PGMA samples together with their deposition conditions.

C. Electron-beam Exposure and Development

After film characterization, PGMA films were sent to the Research Laboratory of Electronics at MIT or shipped to Cornell for exposure and development. To examine the

stability of these films, the sensitivity of each sample was tested one and two weeks after arrival. Electron-beam exposure was carried out using a VS26 scanning-electron-beam lithography tool with acceleration voltage of 50 kV or a Leica/Cambridge EBMF with acceleration voltage of 40 kV. A dosage matrix was used to determine the sensitivity of PGMA films with different molecular weights. After exposure, some films were developed in a 30/70 wt% acetone/isopropanol mixture for 20 secs followed by a N_2 jet; other films were developed in supercritical CO_2 for 10 mins. Supercritical CO_2 development was performed in a supercritical fluid extraction system from Supercritical Fluid Technologies. SCF grade 4.0 liquid CO_2 was introduced into the processing vessel and brought up to a pressure of 5000 psi and a temperature of 45°C. An HPLC pump was used to inject 2 vol% acetone into the fluid as the cosolvent. Scanning electron microscopy (SEM) was done at 5 kV and a current of 1.2 nA using a Leica 440 scanning electron microscope.

Table 3-1. Characteristics of HFCVD PGMA films

Sample	T_f (°C)	Initiator/ precursor	M_n (g/mol)	PDI	Thickness (nm)
1	197	0.6	11,500	1.54	255
2	205	0.9	6,500	2.37	403
3	222	0.9	4,700	2.06	368
4	222	1.2	2,800	1.66	205
5	197	0.9	7,700	2.32	248

3.3 Results and Discussion

A. Film Structure

Figure 3-1 shows the ^1H NMR spectrum of a PGMA film deposited at a filament temperature of 205°C. All the resonance signals are assigned to the corresponding hydrogen atoms in the PGMA chemical structure and summarized in Table 3-2. The chemical shifts at

2.64, 2.86 and 3.24 ppm are assigned to the characteristic resonance signals of PGMA[22], indicating that the epoxy functional group was retained during the process of this low-temperature HFCVD. Furthermore, the peak area ratio obtained from integration of the different signals is in agreement with the number of hydrogen atoms, which verifies that the HFCVD PGMA has the same linear polymeric structure as the solution-polymerized PGMA. Additionally, the ability to completely dissolve the HFCVD film provides evidence of the lack of crosslinking.

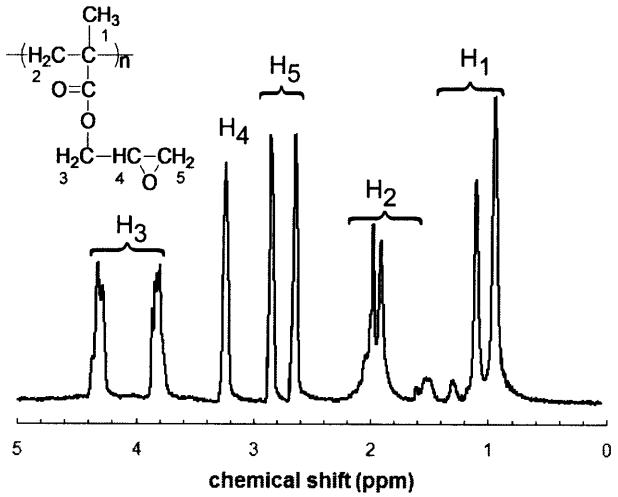

Figure 3-1. ^{1}H NMR spectrum of the HFCVD PGMA film deposited at filament temperature of 205°C. The signal assignments are summarized in Table 3-2, which strongly supports the linear polymer structure and the retention of pendant epoxide rings in the HFCVD films.

Due to the stereoregularity of the PGMA chains, the resonance signals of the $-CH_3$ group split into three different peaks at 1.28 ppm, 1.10 ppm and 0.94 ppm. These three peaks were assigned to the signals of isotactic (mm), heterotactic (mr), and syndiotactic (rr) triads, respectively.[23] Using the molar fractions of tactic sequences calculated from the ^{1}H NMR

spectrum, the fraction of syndiotactic triads in the HFCVD PGMA was estimated to be 76%. The result is close to the syndiotactic percentage (75%) of a PMGA obtained through free radical polymerization in solution[22] and indicates that the polymerization in the HFCVD process produces predominantly syndiotactic polymers.

Table 3-2. ^{1}H NMR chemical shifts and signal assignments of the HFCVD PGMA film

symbol	chemical shift (ppm)	area (arbitrary units)	ref
H_1	0.94, 1.10, 1.28	29.96	23
H_2	1.48-2.02	20.22	23
H_3	4.32, 3.80	20.91	22
H_4	3.24	10.40	22
H_5	2.86, 2.64	20.96	22

B. Film Morphology

Figure 3-2 shows the AFM images of the PGMA films deposited under various filament temperatures with the same initiator/precursor feed ratio 0.9. The PGMA film deposited at a filament temperature of 180 °C shows an undulating morphology with a root-mean-square (rms) roughness of 1.57 nm. As filament temperature increases to 222 °C, the PGMA film becomes much smoother with an rms roughness of 0.3 nm. The power spectral densities (PSD) of the PGMA films show two behaviors. At lower spatial frequencies, the PSD is relatively constant; at higher spatial frequencies, the PSD decays with frequency, which indicates a randomly rough, self-similar surface.[24] By comparison, the calibrating silicon wafer has an rms roughness of 0.2 nm, and the rms roughness of most resists prepared by spin-coating is on the order of ~1 nm.[25] Previous work has shown that fluorocarbon films deposited from HFCVD possess grain structures with high rms roughness.[17] The morphology

difference between HFCVD fluorocarbon films and HFCVD PGMA films is possibly because PGMA chains have a less regular structure and thus lower crystallinity than fluorocarbon polymers. The decrease of film rms roughness with increase of filament temperature is attributed to increasing initiation at higher filament temperatures, which is similar to the phenomenon observed in the deposition of fluorocarbon films.[17]

C. Electron-beam Lithography

Sensitivity curves were obtained by exposing PGMA films to an array of increasing electron-beam dosages and measuring the thickness of the remaining insoluble films after development in acetone. The sensitivity is defined as the dosage required to retain 50% of the original thickness, and the contrast γ is defined as the line slope relating the remaining thickness to the logarithm of the dosage.[26]

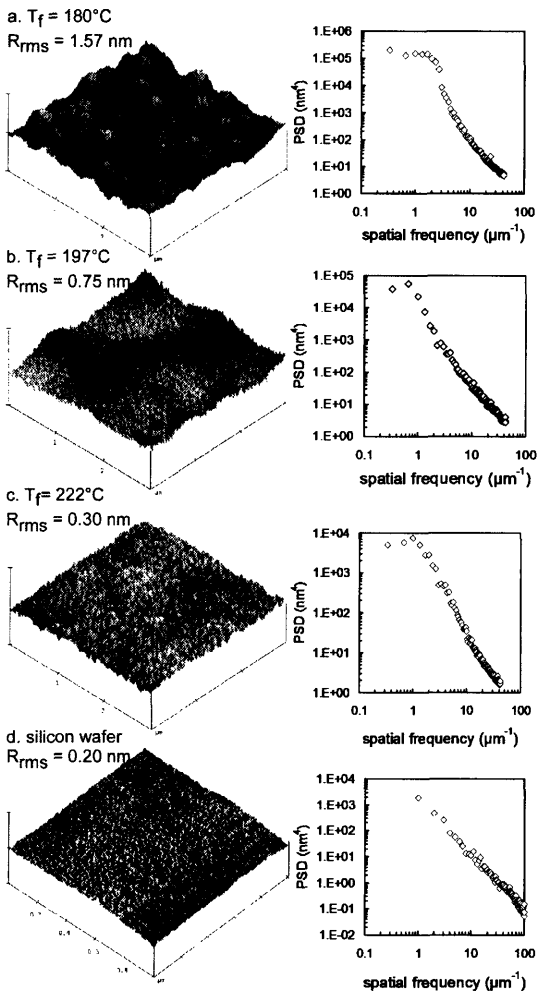

Figure 3-2. Atomic force micrographs showing effect of increasing filament temperature on the morphologies of deposited PGMA films. Films were deposited at an initiator/precursor flow ratio of 0.9 and filament temperatures of (a) 180°C, (b) 197°C, and (c) 222°C. The thickness of films is in the range of 250-360 nm. The morphology of a blank silicon wafer is shown in (d) for comparison. The corresponding 2D isotropic power spectral densities are displayed on the right.

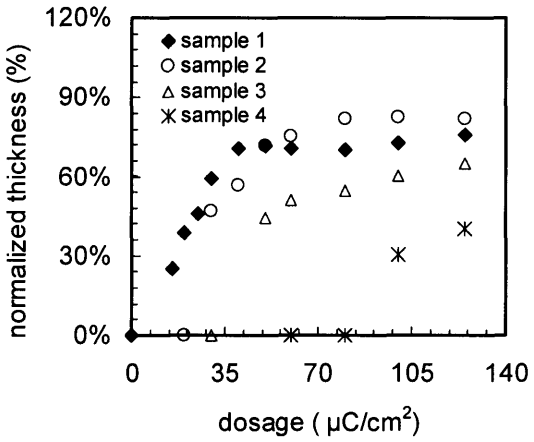

Figure 3-3. Sensitivity curves of sample 1, 2, 3, and 4 using conventional development, showing effect of molecular weight on the electron-beam sensitivity of HFCVD PGMA films. Sample 1 exhibits an electron-beam sensitivity of 27 $\mu C/cm^2$. A PGMA film from solution polymerization and spin-coating with M_n 10,800 g/mol shows an electron-beam sensitivity of 30 $\mu C/cm^2$.

All the PGMA films show minimal aging effect from the results of stability tests described in the experiment section, and a negative-tone feature was obtained for these PGMA films. Sample 1 gave a sensitivity of 27 $\mu C/cm^2$ and a γ value of 1.07; sample 2 gave a sensitivity of 35 $\mu C/cm^2$ and a slightly lower value of γ (0.96) due to its wider molecular weight distribution. The contrast values of HFCVD PGMA films are similar to that of conventional spin-on PGMA.[19] The difference between the sensitivity of these PGMA films and the value reported in literature[20] was attributed to the differences in electron-beam acceleration voltage and film molecular weight. The sensitivity will decrease by more than five times if the electron-beam acceleration voltage increases by a factor of five.[27] As shown in Figure 3-3, sensitivity decreases as the film molecular weight decreases, because a lower-molecular-weight polymer has more chains in a unit volume and requires a higher dosage to

reach a critical crosslink density.[19] By comparison, the PGMA film with M_n 10,800 g/mol prepared from solution polymerization and spin-coating shows an electron-beam sensitivity of 30 μC/cm^2.

A pattern with different feature sizes ranging from 1 μm to sub-0.1 μm was used for resolution testing. Several dosages around the sensitivity were explored to determine the optimal dose for maintaining the feature size in each sample. The minimum feature size obtained in sample 1 is 500 nm, as indicated in Figure 3-4. Smaller features were distorted due to adhesion problems and the swelling phenomenon, which is a common characteristic for negative-tone resists with crosslinking mechanism.[26] The swelling problem can be alleviated by decreasing the film molecular weight, which is demonstrated in sample 5 with 300 nm features achieved. Furthermore, Figure 3-5 shows 200 nm, 100 nm and 80 nm features achieved in sample 3 with number-average molecular weight 4,700 g/mol, but a higher dosage is required due to the effect of molecular weight on sensitivity.

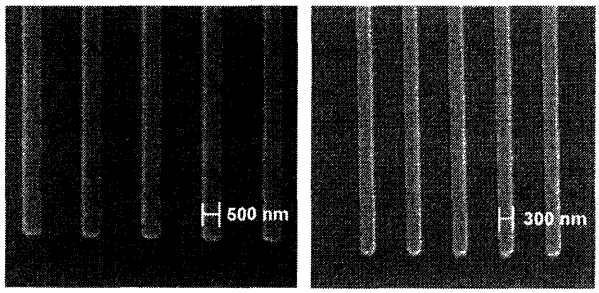

Figure 3-4. Features resolved for samples with different molecular weights using conventional development. Left image shows a 500 nm line pattern for sample 1 exposed at 70 μC/cm^2, right image shows a 300 nm line pattern for sample 5 exposed at 70 μC/cm^2.

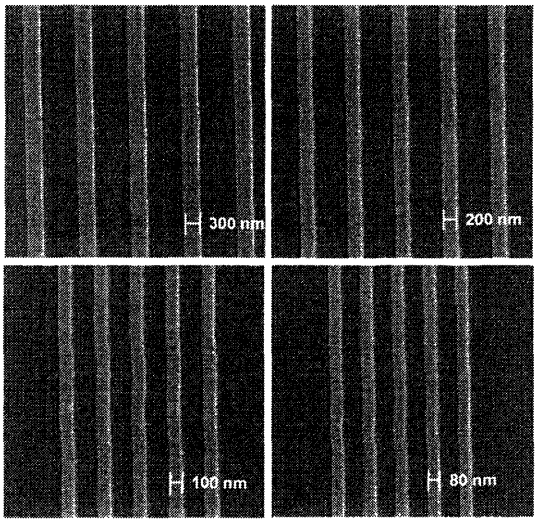

Figure 3-5. SEM photographs showing 300, 200, 100 and 80 nm features achieved in sample 3 exposed at an electron-beam dosage of 100 $\mu C/cm^2$ followed by conventional development.

D. Supercritical CO_2 Processing

Films were also developed using supercritical CO_2 with 2 vol% acetone added as a cosolvent to increase solubility. Incorporation of cosolvents with supercritical CO_2 has been previously utilized for resist stripping.[7] The cosolvent molecules preferentially segregate around the polymer chains, acting similarly to a surfactant.[28] Figure 3-6 shows improved sensitivity of PGMA films using supercritical CO_2 development due to the lower solvating power of the CO_2 mixture than the pure solvent acetone with regard to long polymer chains. For example, sample 1 shows a sensitivity of 15 $\mu C/cm^2$ using supercritical CO_2 compared with the sensitivity of 27 $\mu C/cm^2$ using conventional development. A 300 nm line/space pattern was achieved for sample 3, as indicated in Figure 3-7. Although the necessary dose for retention was about 50 $\mu C/cm^2$, a higher dose of 140 $\mu C/cm^2$ was needed to obtain a high crosslink density to prevent pattern swelling in CO_2 in the 300nm lines. These results

compare favorably to development of inherently CO_2-soluble fluorinated resists. The development conditions with 2 vol% acetone (5000 psi, 45°C) are identical to previous results for fluorinated block copolymers soluble in pure supercritical CO_2.[10] This, in part, illustrates the dramatic effect that cosolvents can have on the solvating power of the supercritical fluid, especially when fluorination of the resist is not a viable option.

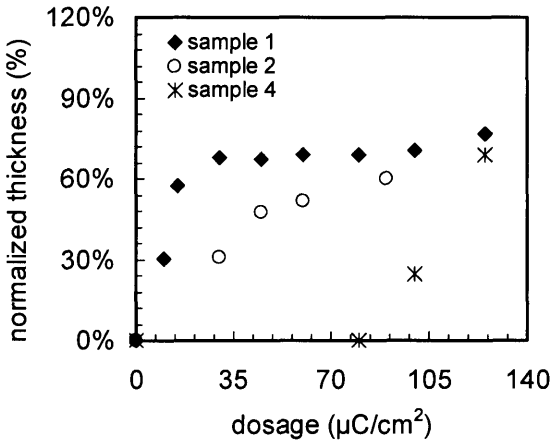

Figure 3-6. Sensitivity curves of sample 1, 2, and 4 using supercritical CO_2 development with 2% acetone added. Sample 1 demonstrates an electron-beam sensitivity of 15 μC/cm^2.

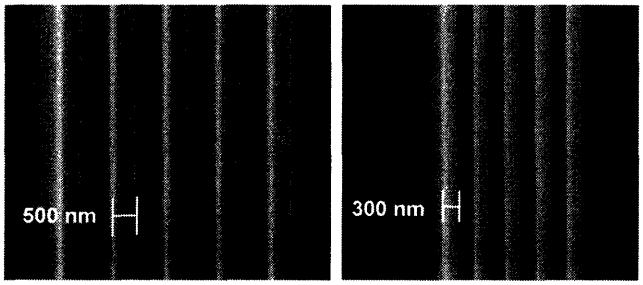

Figure 3-7. 300 and 500 nm line/space patterns achieved for sample 3 exposed at an electron-beam dosage of 140 μC/cm^2 followed by supercritical CO_2 development.

3.4 Conclusions

PGMA thin films were synthesized using HFCVD with retention of pendent epoxide groups and formation of a linear polymeric structure. Film morphology can be controlled by process conditions with rms roughness minimized to 0.3 nm. The PGMA films were investigated as a negative-tone electron-beam resist and demonstrated sensitivity as high as 27 $\mu C/cm^2$ using conventional development. As the molecular weight of the PGMA film decreases, electron-beam sensitivity decreases, but the resolution can be greatly improved by alleviating the swelling problem. The minimum feature size obtained for the PGMA sample with M_n 11,500 g/mol is 500 nm, while the PGMA film with M_n 4,700 g/mol was found to resolve features as small as 80 nm, an improved resolution compared with the 0.16 μm resolution obtained by other negative-tone CVD resists.[5] The patterned PGMA films were also developed using supercritical CO_2 development with 2 vol% acetone added as a cosolvent. A 300 nm line/space pattern was achieved.

As a non-damaging process, the HFCVD process is advantageous over plasma CVD in its capability to avoid crosslinking and retain pendent functionalities. Additionally, HFCVD has the ability to control film molecular weight, which allows optimization of the tradeoff between the improvement of electron-beam sensitivity and the loss of resolution due to swelling. The results presented above indicate the potential of applying this class of HFCVD polymers as "dry" resists. However, the resolution achieved by the HFCVD PGMA is still inferior to that of spin-on resists and needs to be further improved. The ongoing work includes tailoring film properties to improve film adhesion and supercritical CO_2 solubility.

3.5 References

(1) Morita, S.; Tamano, J.; Hattori, S.; Ieda, M. *J. Appl. Phys.* **1980,** *51*, 3938.

(2) Kim, S. O.; Lee, D. C. *Surf. Coat. Technol.* **1999,** *121*, 746.

(3) Horn, M. W.; Pang, S. W.; Rothschild, M. *J. Vac. Sci. Technol. B* **1990,** *8*, 1493.

(4) Horn, M. W.; Rothschild, M.; Maxwell, B. E.; Goodman, R. B.; Kunz, R. R.; Eriksen, L. M. *Appl. Phys. Lett.* **1996,** *68*, 179.

(5) Nalamasu, O.; Wallow, T. I.; Reichmanis, E.; Novembre, A. E.; Houlihan, F. M.; Dabbagh, G.; Mixon, D. A.; Hutton, R. S.; Timko, A. G.; Wood, O. R.; Cirelli, R. A. *Microelectron. Eng.* **1997,** *35*, 133.

(6) Wolf, S.; Tauber, R. N. *Silicon Processing for the VLSI Era.* 2nd ed.; Lattice Press: Sunset Beach, 2000.

(7) Weibel, G. L.; Ober, C. K. *Microelectron. Eng.* **2003,** *65*, 145.

(8) Kirby, C. F.; McHugh, M. A. **1999,** *99*, 565.

(9) McHugh, M. A.; Krukonis, V. J. *Supercritical Fluid Extraction: Principles and Practice.* 2nd ed.; Butterworth: Boston, 1994.

(10) Gallagher-Wetmore, P.; Wallraff, G. M.; Allen, R. D. **1995,** *2438*, 694.

(11) Sundararajan, N.; Yang, S.; Ogino, K.; Valiyaveettil, S.; Wang, J. G.; Zhou, X. Y.; Ober, C. K.; Obendorf, S. K.; Allen, R. D. **2000,** *12*, 41.

(12) Ruckenstein, E.; Shulgin, I. **2001,** *180*, 345.

(13) Lee, L. S.; Gleason, K. K. *Electrochem. Solid State Lett.* **2001,** *4*, G81.

(14) Lau, K. K. S.; Caulfield, J. A.; Gleason, K. K. *Chem. Mat.* **2000,** *12*, 3032.

(15) Lewis, H. G. P.; Casserly, T. B.; Gleason, K. K. *J. Electrochem. Soc.* **2001,** *148*, F212.

(16) Murthy, S. K.; Olsen, B. D.; Gleason, K. K. *Langmuir* **2002,** *18*, 6424.

(17) Lewis, H. G. P.; Caulfield, J. A.; Gleason, K. K. *Langmuir* **2001,** *17*, 7652.

(18) Mao, Y.; Gleason, K. K. *Langmuir* **2004,** *20*, 2484.

(19) Thompson, L. F. *Solid State Technol.* **1974,** *17*, 41.

(20) Thompson, L. F.; Feit, E. D.; Heidenreich, R. D. *Polym. Eng. Sci.* **1974,** *14*, 529.

(21) Lau, K. K. S.; Murthy, S. K.; Lewis, H. G. P.; Caulfield, J. A.; Gleason, K. K. *J. Fluor. Chem.* **2003,** *122*, 93.

(22) Gromada, M.; le Pichon, L.; Mortreux, A.; Leising, F.; Carpentier, J. F. *J. Organomet. Chem.* **2003,** *683*, 44.

(23) Espinosa, M. H.; del Toro, P. J. O.; Silva, D. Z. *Polymer* **2001,** *42*, 3393.

(24) Buchko, C. J.; Kozloff, K. M.; Martin, D. C. *Biomaterials* **2001,** *22*, 1289.

(25) Sakamizu, T.; Shiraishi, H. *Microelectron. Eng.* **2002,** *61-2*, 763.

(26) Thompson, L. F.; Willson, C. G. *Introduction to Microlithography*. 2nd ed.; American Chemical Society: Washington, DC, 1994.

(27) Medeiros, D. R.; Aviram, A.; Guarnieri, C. R.; Huang, W. S.; Kwong, R.; Magg, C. K.; Mahorowala, A. P.; Moreau, W. M.; Petrillo, K. E.; Angelopoulos, M. *IBM J. Res. Dev.* **2001,** *45*, 639.

(28) Zhang, X. G.; Han, B. X.; Hou, Z. S.; Zhang, H. L.; Liu, Z. M.; Jiang, T.; He, J.; Li, H. P. **2002,** *8*, 5107.

CHAPTER FOUR

Positive-tone Nanopatterning of Chemical Vapor Deposited Thin Films

Y. Mao and K. K. Gleason, submitted to *Langmuir.*

Abstract

Terpolymers of methyl α-chloroacrylate (MCA), methacrylic acid (MAA), and methacrylic anhydride (MAH) were synthesized by initiated chemical vapor deposition (iCVD) of MCA and MAA followed by low-temperature annealing that partially converts MAA into MAH. The MAA composition in the iCVD copolymer can be systematically varied between 37 mol% and 85 mol% by adjusting the gas feed fractions of monomers. Study of the monomer reactivity ratios and the copolymer molecular weights supports the hypothesis of a surface propagation mechanism during the iCVD copolymerization. The carboxylic dehydration reaction at the annealing temperature of 160°C is dominated by a mechanism of intramolecular cyclization, resulting in intramolecular MAH anhydride formation while preventing crosslink formation. The incorporation of highly electron-withdrawing anhydride functionality enhances chain scission susceptibility under electron-beam irradiation. P(MCA-MAA-MAH) terpolymer thin films can be completely developed at dosage as low as 20 $\mu C/cm^2$ at 50 kV. High-quality positive-tone patterns were created with 60 nm feature size achieved.

Acknowledgements

We gratefully acknowledge the support of the NSF/SRC Engineering Research Center for Environmentally Benign Semiconductor Manufacturing. This work made use of MIT's shared scanning-electron-beam-lithography facility in the Research Laboratory of Electronics.

4.1 Introduction

The continued miniaturization of electronic and sensor structures towards nanometer scales has prompted creative research on patterning. Conventional lithography includes fabricating polymer thin films using spin-on coating and subsequent exposure and development.[1] Although it is the dominant technology, new ideas is required to deal with problems such as nonplanarity in substrates and formation of three-dimensional microstructures.[2] Soft lithography[3] and imprint lithography[4] have been extensively investigated, aiming to replace the traditional lithographic patterning. Another alternative is to replace the traditional "wet" spin-on method for thin film fabrication with a "dry" chemical vapor deposition (CVD) method. The conformal nature of the CVD process would enable patterning on substrates with complex geometries.[5] Combined with microcontact printing, CVD has been used in patterning of nonplanar substrates.[6] The vapor phase processing method can easily fabricate thin films on plastic substrates and thus has the flexibility to be integrated into a wider range of new material applications.[7] The vacuum process of CVD allows production of cleaner surfaces with macroscale uniformity and extremely small roughness.[8] The all dry process is also desirable because of increasing concern about environmental issues.

There are two criteria in evaluating a lithography process, resolution and sensitivity. Electron-beam lithography provides high resolution.[9] Solution-polymerized poly(methyl methacrylate) (PMMA) is the benchmark in the development of electron-beam imaging materials. PMMA undergoes chain scission upon electron-beam exposure, resulting in reduction of molecular weight and a positive-tone image after development.[9] High-molecular-weight PMMA has been shown to create 20 nm feature sizes.[10] However, it

requires high dosage (> 40 $\mu C/cm^2$ at an acceleration voltage of 15 kV and >300 $\mu C/cm^2$ at 50 kV) to produce small features. PMMA derivatives with highly electron-withdrawing side groups have been investigated to improve the sensitivity. Among them, poly(methyl α-chloroacrylate) (PMCA) was reported to undergo chain scission at electron-beam dosages of 15 $\mu C/cm^2$ at 15 kV.[11,12] Copolymerizations of MCA with methacrylonitrile,[13] trihaloethylmethacrylate,[14] and methacrylic acid[15] have been explored with images of 1 μm in size demonstrated. Introduction of poly(methacrylic anhydride) (PMAH) also improves chain scission propensity with an electron-beam sensitivity of 7 $\mu C/cm^2$ reported at 15 kV.[16] But insoluble byproducts were produced during the anhydride formation at 220°C, and the thin film fabrication requires several steps, including synthesis, baking, dissolving, filtration, and spin-on coating.

Efforts have been made to incorporate CVD thin film fabrication as part of a dry lithography process.[17,18] Plasma polymerized PMMA was explored with patterns demonstrated using an electron-beam dosage of 160 $\mu C/cm^2$ at 20 kV.[19] Linear poly(glycidyl methacrylate) (PGMA) thin films have been deposited using initiated chemical vapor deposition (iCVD).[8] Features of 80 nm have been achieved under a dosage of 70 $\mu C/cm^2$ at 50 kV. However, swelling of small features was observed due to the crosslinking mechanism used in creating the pattern, a problem often encountered in negative-tone imaging materials.[20] In order to produce high-quality patterns, a positive-tone imaging material not requiring crosslinking chemistry needs to be explored. In addition, low irradiation dosage is desired because of electron forward scattering.[20]

In this paper, we use iCVD copolymerization and low-temperature annealing to combine anhydride chemistry with MCA chemistry. The goal is to create an environmentally friendly, simple approach for production of high-quality patterns. Since there is little research

about vapor-phase copolymerization of vinyl monomers, we will investigate the chemistry of the iCVD synthesis in detail. We will also discuss the formation of anhydride chemistry during low-temperature annealing and the exposure chemistry of the post-annealed thin films.

4.2 Experimental Methods

Films were deposited onto silicon wafer substrates in a custom-built reactor. The reactor was equipped with a stainless steel filament array and a water-cooled stage on which the substrates were placed. The temperature of the stage was varied between 6°C to 25°C. The filament was resistively heated to 250°C to thermally decompose the initiator and generate radicals. Both the initiator tert-butyl peroxide and the monomer methyl α-chloroacrylate (MCA) were obtained from Aldrich and vaporized at room temperature. The second monomer methacrylic acid (MAA, Aldrich) was vaporized in a glass jar heated to 70°C. The flow rate of peroxide was regulated using a mass flow controller and kept constant at 0.4 sccm, while the flow rates of MCA and MAA were varied between 0.2 and 2.7 sccm using needle valves. All vapors were mixed together before entering the reactor through a side port. Pressure in the vacuum chamber was maintained at 0.8 torr. Other experimental set-up details have been described previously.[8]

Fourier transform infrared (FTIR) measurements were done on a Nicolet Nexus 870 spectrometer in transmission mode using a DTGS KBr detector over the range of 400-4000 cm^{-1} at 4 cm^{-1} resolution. Film molecular weight was measured using gel permeation chromatography with a Waters 1525 Binary HPLC pump equipped with two columns from Waters. Polystyrene standards (Aldrich) were used for calibration, and tetrahydrofuran was used as the eluent.

The copolymer thin films were annealed at 160°C for 60 mins in vacuum. Electron-beam exposure was carried out using a VS26 scanning-electron-beam lithography tool with acceleration voltage of 50 kV. After exposure, films were developed in solutions of isopropanol and dimethylacetamide with volume mix ratio 5:1 and 5:2. A dosage matrix was used to determine the minimum dosage for complete development of the post-annealed films. Film thickness was measured using profilometry. A pattern with feature size ranging from 500 nm to 50 nm was used for the electron-beam writing. Scanning electron microscopy (SEM) was done at 15 kV using a FEI/Philips XL30 FEG scanning electron microscope.

4.3 Results and Discussion

Deposition Chemistry. P(MCA-MAA) copolymer thin films with varying compositions were synthesized by adjusting the feed fractions of monomers MCA and MAA during iCVD. Figure 4-1 shows the FTIR spectra of three iCVD copolymers compared with the spectra of the iCVD homopolymers PMCA and PMAA. There are four types of absorption peaks: C=O stretching in -COOH (1702 cm^{-1}),[21,22] C=O stretching in α-chloroacrylate (1732 and 1761 cm^{-1}),[23] C-H stretching (2800-3100 cm^{-1}), and O-H stretching in –COOH (3000-3500 cm^{-1}). The –COOH absorption at 1702 cm^{-1} indicates a predominantly syndiotactic stereoregularity,[24] which is typical in iCVD free radical polymerizations.[8] The presence of absorption peaks at 1702, 1732, and 1761 cm^{-1} proves the successful retention of carboxylic acid and ester groups. With the increase of the MAA feed fraction, the intensity of the carboxylic and the hydroxyl absorptions increases, indicating more MAA content incorporated into the copolymer.

The composition of P(MCA-MAA) copolymers can be quantitatively analyzed using the method of curve fitting within the carbonyl stretching region.[21,22] The resulting MAA mole fraction (F_A) is plotted versus the MAA feed mole fraction (f_A) in Figure 4-2a, demonstrating the systematic tuning of film composition during iCVD. The first-order Markov model relates the copolymer composition to monomer mole fraction through the copolymerization equation,[25] which can be rearranged into:

$$\frac{f_A(1-2F_A)}{F_A(1-f_A)} = r_B + \left[\frac{f_A^2(F_A-1)}{F_A(1-f_A)^2}\right] r_A$$

where r_A is the reactivity ratio of MAA, and r_B is the reactivity ratio of MCA. Thus the monomer reactivity ratios can be determined from the plot of $\frac{f_A(1-2F_A)}{F_A(1-f_A)}$ versus $\frac{f_A^2(F_A-1)}{F_A(1-f_A)^2}$, as shown in Figure 4-2b. r_A is estimated to be 6.02 from the slope of the least-squares linear regression of the data, and r_B is estimated to be 0.18 from the intercept. The theoretical values of r_A and r_B in MCA and MAA copolymerization can also be calculated according to the Q-e scheme.[26] Based on the Q and e values of MCA and MAA[26] (Q_{MAA} = 1.38, e_{MAA} = 0.59, Q_{MCA} = 1.68, e_{MCA} = 0.51), r_A is calculated to be 0.78, and r_B is calculated to be 1.27. The difference between the iCVD reactivity ratios and the theoretical values is possibly due to the discrepancy between the iCVD gas mole fraction and the mole fraction at the actual propagation site. It has been postulated that vinyl monomers polymerize through three steps during iCVD: initiation, propagation, and termination.[27] Most likely, initiation will occur in the heated vapor phase region around the filaments, while propagation can take place either in the vapor phase or on the cooled substrate surface. In the case of surface propagation, the surface mole fraction of MAA is higher than its gas mole fraction,

because MAA (equilibrium vapor pressure $P_{A,0}$= 1.23 torr at 25°C) is less volatile than MCA ($P_{B,0}$ = 12.6 torr at 25°C) and has a higher tendency to adsorb to the surface. Therefore the calculation based on the lower gas mole fraction gives a higher apparent reactivity ratio of MAA. Using the relationship between monomer pressure and monomer surface concentration in the modeling of xylylene vapor polymerization,[28] the MAA surface concentration $f_A^{'}$ can be calculated using:

$$f_A^{'} = \frac{P_t f_A / P_{A,0} M_A}{P_t f_A / P_{A,0} M_A + P_t (1 - f_A) / P_{B,0} M_B}$$

where P_t is the total pressure during deposition, M_A is the molecular weight of MAA, and M_B is the molecular weight of MCA. The plot of $\frac{f_A^{'}(1-2F_A)}{F_A(1-f_A^{'})}$ versus $\frac{(f_A^{'})^2(F_A-1)}{F_A(1-f_A^{'})^2}$ gives a new set of reactivity ratios: $r_A^{'} = 0.41, r_B^{'} = 2.05$, which are close to the theoretical values and support the hypothesis of a surface polymerization mechanism.

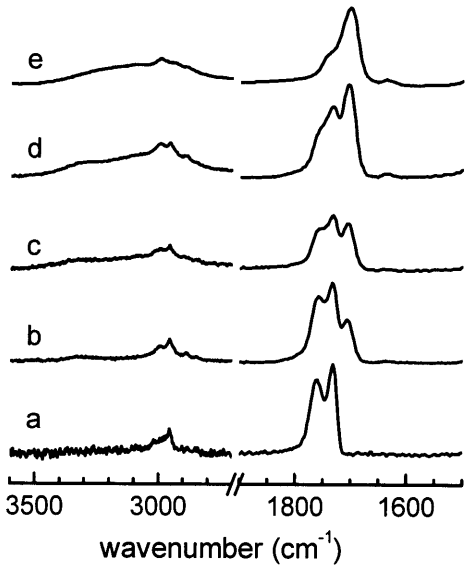

Figure 4-1. FTIR spectra of iCVD PMCA homopolymer (a), P(MCA-MAA) copolymer with MAA feed fraction 0.08 (b), 0.21 (c), 0.34 (d), and PMAA (e).

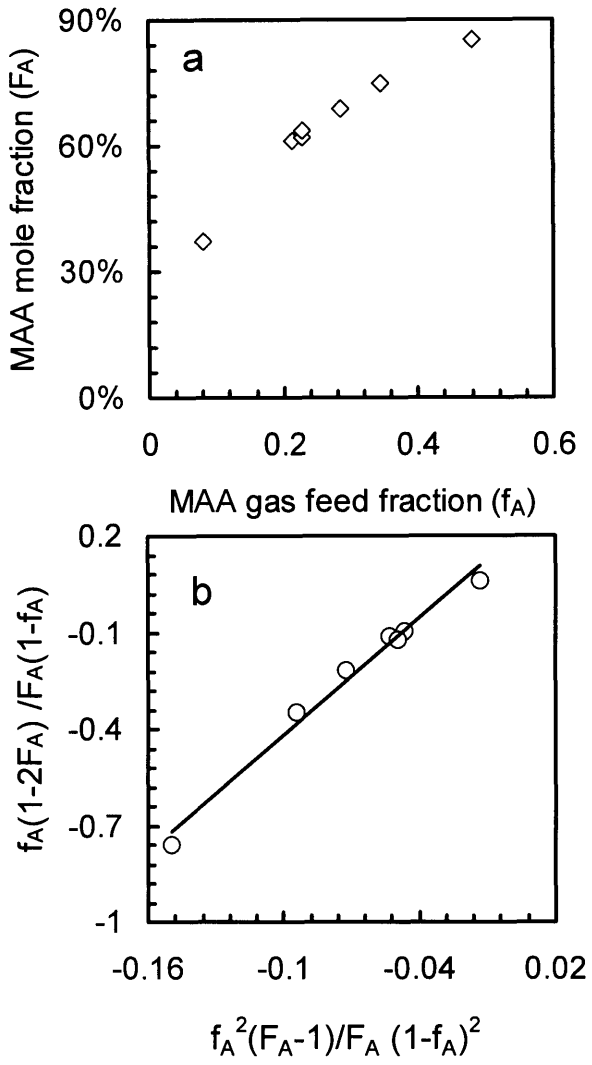

Figure 4-2. Systematic tuning of copolymer film composition during iCVD. A) relationship between MAA mole fractions in P(MCA-MAA) copolymers and MAA gas feed fractions; and B) plot of the rearranged copolymerization equation, which gives the estimation of monomer reactivity ratios: $r_A = 6.02$, $r_B = 0.18$.

Additionally, the molecular weight of copolymer thin films can be easily controlled by adjusting the surface temperature during the iCVD process, as shown in Figure 4-3. With

other deposition parameters fixed, the weight-average molecular weight M_w increases as the surface temperature drops. Again, the trend of increasing M_w with decreasing surface temperature is consistent with the surface polymerization mechanism for iCVD. In the scenario of surface propagation, decreasing surface temperature favors adsorption of both short-chain radicals and monomers, resulting in increasing concentration of reactive species, and thus increasing chain length.[25] In the scenario of vapor-phase propagation, however, it is expected that changing surface temperature from 6°C to 25°C has minimal effect on the vapor phase kinetics. Therefore it will not affect the growth of long-chain radicals and the M_w of thin films to any large extent.

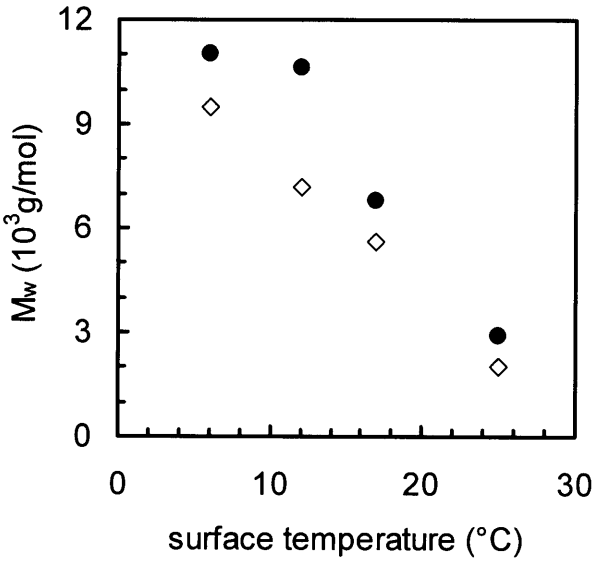

Figure 4-3. Effect of surface temperature during iCVD on the molecular weight of P(MCA-MAA) copolymer thin films with original MAA compositions 75-77 mol% (•) and 40-44 mol% (◊).

Annealing Chemistry. Neighboring carboxylic acids undergo dehydration reaction at elevated temperatures, resulting in the formation of anhydrides.[21,29] The dehydration in P(MCA-MAA) copolymers can occur either intermolecularly to produce an open-chain methacrylic anhydride (MAH), or intramolecularly to form a cyclic MAH, producing P(MCA-MAA-MAH) terpolymers, as indicated in Scheme 1. In this work, a low annealing temperature of 160°C was chosen to minimize the intermolecular reaction and crosslink formation. Figure 4-4 shows the FTIR spectra of a P(MCA-MAA) copolymer before and after annealing. The original MAA composition of the copolymer is 76 mol%. After annealing, two new absorption peaks appear at 1760 and 1785 cm^{-1}, which are assigned to the C=O stretching in cyclic and open-chain anhydrides, respectively.[30] The intensity difference between these two absorption peaks indicates that carboxylic dehydration at 160°C is dominated by a mechanism of intramolecular cyclization. The conversion of carboxylic groups to anhydrides can be further confirmed through the appearance of C-O-C stretching vibration[24] at 1021 cm^{-1} and the intensity decrease of C=O absorption in COOH at 1702 cm^{-1}. The carbonyl ester stretching in the α-chloroacrylate overlaps with other carbonyl absorptions and becomes almost invisible as a shoulder.

Scheme 1

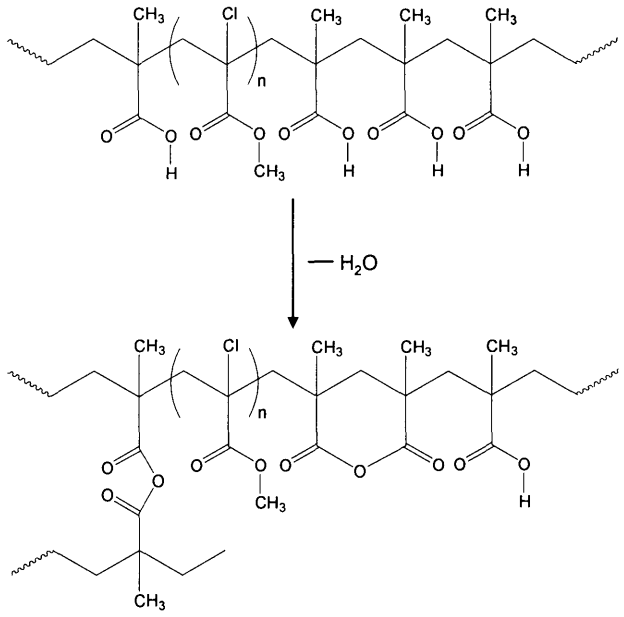

The molecular weights and molecular weight distributions of P(MCA-MAA) copolymers before and after annealing are summarized in Table 4-1. A slight increase of M_w is observed after annealing, which further confirms the low degree of intermolecular anhydride formation detected from the C=O absorption intensity difference between intramolecular and intermolecular anhydride in Figure 4-4. The existence of only a small amount of anhydride linkages between adjacent polymer chains enables subsequent thin film exposure and development to be carried out without requiring removal of insoluble byproducts. The ratio of molecular weight improvement after annealing, $M_{w,f}/M_{w,i}$, improves with the increase of MAA content, a consequence of a greater number of MAA units along copolymer chains. The polydispersity index (PDI) of as-deposited copolymers is in the range of 1.3-2.2. This narrow molecular weight distribution suggests low monomer conversion during the free radical polymerization.[25] Increase of PDI upon annealing is possibly because

longer-chain species have more MAA units, and thus higher intermolecular reaction tendency, than shorter-chain species.

Table 4-1. M_w and PDI of P(MCA-MAA) copolymers after annealing.

	as deposited		after annealing		
MAA content (%)	$M_{w,i}$ (10^3g/mol)	PDI	$M_{w,f}$ (10^3 g/mol)	PDI	$M_{w,f}$/ $M_{w,i}$
40-44	2.0	1.33	2.3	1.47	1.15
	5.6	1.70	6.4	1.93	1.14
	9.5	2.06	11.2	2.28	1.18
60-62	3.9	1.54	4.3	1.65	1.10
	6.5	1.89	8.1	2.32	1.25
75-77	2.9	1.54	3.1	1.60	1.08
	6.8	1.47	9.2	1.96	1.35
	10.6	2.21	15.6	3.01	1.47

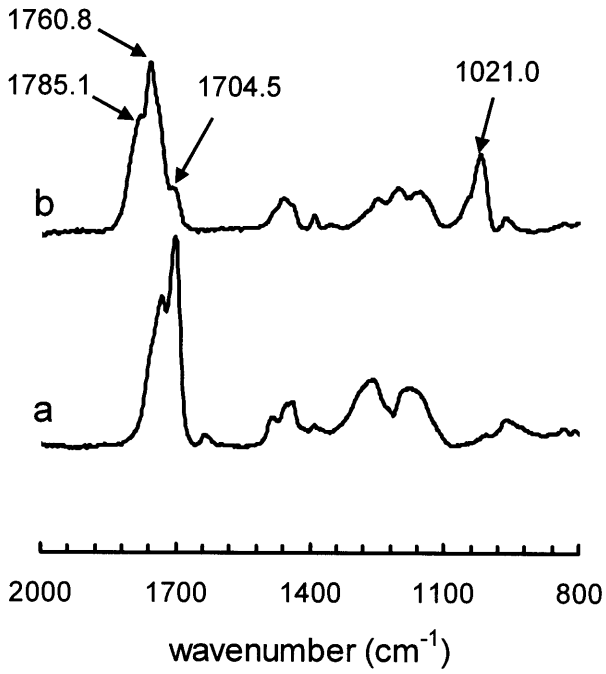

Figure 4-4. FTIR spectra of P(MCA-MAA) copolymer thin films with original MAA composition 76% before (a) and after annealing at 160°C for 60 mins (b).

Exposure Chemistry. Similarly to PMMA, P(MCA-MAA-MAH) terpolymer undergoes a free radical depolymerization pathway upon electron-beam irradiation, as shown in Scheme 2. The depolymerization results in low-molecular-weight fragments with high solubility in a developer. Figure 4-5 shows the minimum clearing dosage of terpolymers with different original MAA compositions. The terpolymer with original MAA composition 75% and M_w 10.6 kg/mol can be completely developed at dosage as low as 20 $\mu C/cm^2$ at 50 kV. By comparison, development of high-molecular-weight PMMA requires dosage > 40 $\mu C/cm^2$ at 15 kV,[20] and the development dosage is estimated to increase more than three times if the acceleration voltage increases by a factor of three.[9] The low clearing dosage is attributed to the enhanced chain scission susceptibility over PMMA, because both chlorine and anhydride are highly electron-withdrawing groups and provide stabilization to free radical intermediates during chain scission. In addition, the incorporation of anhydride modifies the terpolymer degradation chemistry by introducing a molecular depolymerization mechanism yielding olefin and ketene end groups.[31] The molecular mechanism has been estimated to be eight times more efficient than the free radical mechanism in creating chain scission in PMAH, which contributes to more than 50% improvement in the chain scission propensity in PMAH compared with PMCA.[31,32] This effect is also exemplified in Figure 4-5: terpolymers with higher original MAA composition require lower dosage for complete development. The clearing dosage increases as the film molecular weight decreases, because a lower-molecular-weight polymer has more chains and requires more breakages in a unit volume to create the solubility difference.

Scheme 2

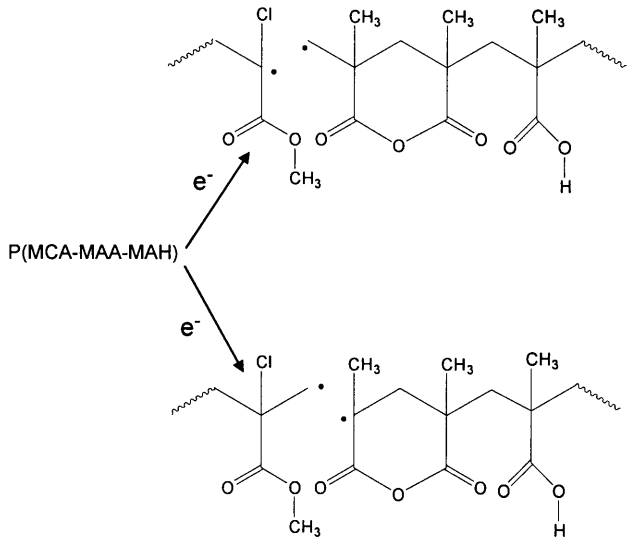

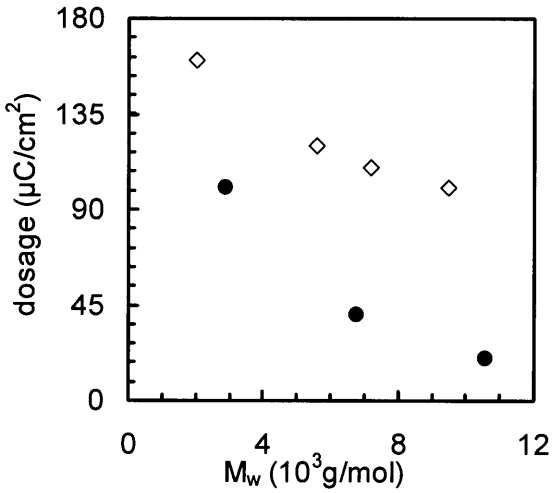

Figure 4-5. Minimum dosage required for complete development of post-annealed P(MCA-MAA) copolymer thin films with original MAA compositions 75-77 mol% (•) and 40-44 mol% (◊).

After the terpolymer depolymerizes in the exposed region, subsequent development removes all the fragments in this region while leaving the unexposed area intact, thus creating a positive-tone pattern. This positive-tone mechanism eliminates the swelling problem

typically encountered in negative-tone patterns bearing a crosslinking mechanism.[20] It is the positive-tone mechanism combined with the improved irradiation sensitivity of the terpolymer that enables high-quality patterns to be created at small dimensions. As can be seen in Figure 4-6, patterns without deformation can be clearly achieved at 60 nm resolution in the terpolymer with original MAA composition 75% and M_w 6.8 kg/mol.

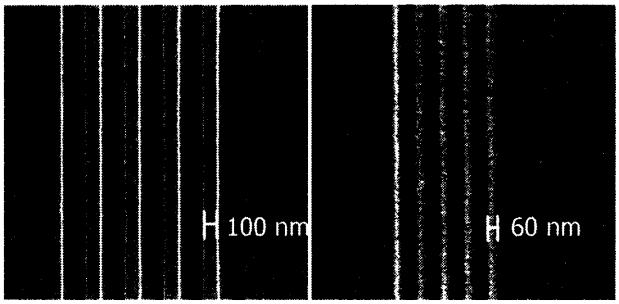

Figure 4-6. 100 nm and 60 nm features achieved in the terpolymer with original MAA composition 75% and M_w 6.8 kg/mol.

4.4 Conclusions

P(MCA-MAA) copolymer thin films were synthesized using iCVD with pendant functional groups retained. The composition (MAA 37-85 mol%) and molecular weight (M_w 2.0-11.2 kg/mol) of the copolymer can be systematically controlled by adjusting the iCVD process parameters. The study of copolymerization reactivity ratios and the effect of process parameters on copolymer molecular weights indicate a surface propagation pathway during iCVD. Annealing of the P(MCA-MAA) thin films at 160°C is dominated by intramolecular anhydride formation, which prevents crosslink formation within the thin films and allows subsequent patterning to be carried out directly. Highly electron-withdrawing anhydride functionalities were incorporated into the thin films after annealing and enhance chain scission susceptibility under electron-beam irradiation. The post-annealed P(MCA-MAA)

copolymer thin films can be completely developed at dosage as low as 20 $\mu C/cm^2$ at 50 kV. High-quality positive-tone patterns were created with 60 nm feature size achieved.

4.5 References

(1) Sundararajan, N.; Yang, S.; Ogino, K.; Valiyaveettil, S.; Wang, J. G.; Zhou, X. Y.; Ober, C. K.; Obendorf, S. K.; Allen, R. D. *Chem. Mat.* **2000,** *12*, 41.

(2) Xia, Y. N.; Whitesides, G. M. *Annu. Rev. Mater. Sci.* **1998,** *28*, 153.

(3) Xia, Y.; Whitesides, G. M. *Science* **1996,** *37*, 85.

(4) Chou, S. Y.; Krauss, P. R.; Renstrom, P. J. *Science* **1996,** *272*, 85.

(5) Pierson, H. O. *Handbook of Chemical Vapor Deposition.* 2nd ed.; Noyes Publications: Norwich, NY, 1999.

(6) Jeon, N. L.; Nuzzo, R. G.; Xia, Y. N.; Mrksich, M.; Whitesides, G. M. *Langmuir* **1995,** *11*, 3024.

(7) Forrest, S. R. *Nature* **2004,** *428*, 911.

(8) Mao, Y.; Felix, N. M.; Nguyen, P. T.; Ober, C. K.; Gleason, K. K. *J. Vac. Sci. Technol. B* **2004,** *22*, 2473.

(9) Medeiros, D. R.; Aviram, A.; Guarnieri, C. R.; Huang, W. S.; Kwong, R.; Magg, C. K.; Mahorowala, A. P.; Moreau, W. M.; Petrillo, K. E.; Angelopoulos, M. *IBM J. Res. Dev.* **2001,** *45*, 639.

(10) Broers, A. N. **1981,** *128*, 166.

(11) Helbert, J. N.; Chen, C. Y.; Pittman, C. U.; Hagnauer, G. L. *Macromolecules* **1978,** *11*, 1104.

(12) Helbert, J. N.; Cook, C. F.; Poindexter, E. H. *J. Electrochem. Soc.* **1977,** *124*, 158.

(13) Lai, J. H.; Helbert, J. N.; Cook, C. F.; Pittman, C. U. **1979,** *16*, 1992.

(14) Babu, G. N.; Lu, P. H.; Hsu, S. L.; Chien, J. C. W. *J. Polym. Sci. Pol. Chem.* **1984,** *22*, 195.

(15) Lai, J. H.; Shepherd, L. T. *J. Electrochem. Soc.* **1982,** *129*, C109.

(16) Moreau, W.; Merritt, D.; Moyer, W.; Hatzakis, M.; Johnson, D.; Pederson, L. **1979,** *16*, 1989.

(17) Nalamasu, O.; Wallow, T. I.; Reichmanis, E.; Novembre, A. E.; Houlihan, F. M.; Dabbagh, G.; Mixon, D. A.; Hutton, R. S.; Timko, A. G.; Wood, O. R.; Cirelli, R. A. *Microelectron. Eng.* **1997,** *35*, 133.

(18) Horn, M. W.; Pang, S. W.; Rothschild, M. *J. Vac. Sci. Technol. B* **1990,** *8*, 1493.

(19) Morita, S.; Tamano, J.; Hattori, S.; Ieda, M. *J. Appl. Phys.* **1980,** *51*, 3938.

(20) Thompson, L. F.; Willson, C. G. *Introduction to Microlithography*. 2nd ed.; American Chemical Society: Washington, DC, 1994.

(21) Lee, J. Y.; Painter, P. C.; Coleman, M. M. *Macromolecules* **1988,** *21*, 346.

(22) Dong, J.; Tsubahara, N.; Fujimoto, Y.; Ozaki, Y.; Nakashima, K. *Appl. Spectrosc.* **2001,** *55*, 1603.

(23) Hummel, D. O.; Scholl, F. *Atlas of Polymer and Plastics Analysis*. 2nd ed.; Carl Hanser Verlag: Munich, 1978.

(24) Lazzari, M.; Kitayama, T.; Hatada, K.; Chiantore, O. *Macromolecules* **1998,** *31*, 8075.

(25) Odian, G. *Principles of Polymerization*. 2nd ed.; Wiley-Interscience: New York, 1981.

(26) Greenley, R. Z. **1975,** *A 9*, 505.

(27) Mao, Y.; Gleason, K. K. *Langmuir* **2004,** *20*, 2484.

(28) Beach, W. F. **1978,** *11*, 72.

(29) Maurer, J. J.; Eustace, D. J.; Ratcliffe, C. T. *Macromolecules* **1987,** *20*, 196.

(30) Bellamy, L. J. *The Infrared Spectra of Complex Molecules*. 1st ed.; Chapman and Hall: London, 1975.

(31) Hiraoka, H. *IBM J. Res. Dev.* **1977,** *21*, 121.

(32) Chen, C. Y.; Pittman, C. U.; Helbert, J. N. *J. Polym. Sci. Pol. Chem.* **1980,** *18*, 169.

CHAPTER FIVE

Chemical Vapor Deposited Polyacrylic Thin Films Patterned Using E-beam and Supercritical CO_2

Y. Mao, N. M. Felix, P. T. Nguyen, C. K. Ober, K. K. Gleason, submitted to *Chemical Vapor Deposition.*

Abstract

We investigated using initiated chemical vapor deposition (iCVD) copolymerization to incorporate fluorinated acrylics into poly(glycidyl methacrylate) (PGMA) and poly(methacrylic acid) (PMAA) thin films. The fluorinated acrylics greatly improve the supercritical (sc) CO_2 solubility of hydrocarbon polymers. The crosslinking chemistry of the GMA component creates a negative-tone contrast after e-beam exposure, while the chain scission chemistry in post-annealed fluorinated PMAA thin films forms non-swelling positive-tone images. Features of 300 nm were obtained using $scCO_2$ development in both types of thin films. The performance of two fluorinated acrylics was also evaluated. These results demonstrate potential of applying these iCVD thin films as "dry" resists by eliminating the wet chemistry during the deposition and the development steps.

Acknowledgements

We gratefully acknowledge the support of the NSF/SRC Engineering Research Center for Environmentally Benign Semiconductor Manufacturing. This work made use of MIT's shared scanning-electron-beam-lithography facility in the Research Laboratory of Electronics (SEBL at RLE), MRSEC Shared Facilities supported by the National Science Foundation under Award Number DMR-9400334, and the Cornell Nanoscale Facility.

5.1 Introduction

Motivated by both the desire to improve lithographic performance and to reduce environmental impact, resist development by supercritical CO_2 ($scCO_2$) has gained considerable attention.[1-3] $scCO_2$ is envisioned as an "environmentally responsible" solvent and is widely used in food and pharmaceutical industries.[4] $scCO_2$ also has unique properties beneficial for the development of dense, high-aspect-ratio, submicron features: high diffusivity, high density, low viscosity, and the absence of surface tension, which prevents pattern collapse.[5]

Additionally, chemical vapor deposition (CVD) has the potential to eliminate the solvent for applying resists[6-8] by combining polymer synthesis and thin film coating into one single step. Patterning of CVD thin films using $scCO_2$ development was first explored in CVD poly(tetrafluoroethylene) (PTFE) thin films.[9] Positive-tone contrast was obtained after e-beam exposure with a dosage of 6000 $\mu C/cm^2$ followed by $scCO_2$ development. Lines/spaces pattern of 1.0 μm was achieved. However, the dosage required for development of PTFE is two orders of magnitude higher than the dosage of common e-beam resists,[10] which suggests that moieties more sensitive to e-beam needs to be incorporated. Mild CVD conditions are required in order to avoid side reactions and thus retain the delicate organic functionalities typically needed for lithographic chemistries.[11] Initiated chemical vapor deposition (iCVD) permits reaction at mild process conditions[12] ($T < 200°C$, energy input 3 W) through thermal decomposition of an initiator and subsequent addition reaction of monomer species. In addition, iCVD copolymerization provides an approach to further tune film composition and properties for specific applications.[13]

Poly(glycidyl methacrylate) (PGMA) thin films and terpolymers of methyl α–

chloroacrylate (MCA), methacrylic acid (MAA), and methacrylic anhydride (MAH) have been successfully synthesized using iCVD.[13,14] Both negative-tone and positive-tone contrast have been demonstrated after e-beam exposure and conventional wet development. The primary challenge in using $scCO_2$ for the development of these polymers arises from the fact that these materials have low solubility in $scCO_2$.[15]

The $scCO_2$ solubility of polymers is a function of both the backbone stiffness and the side group compositions. Acrylic fluoropolymers, which contain a lipophilic acrylate backbone and a CO_2-philic, fluorinated side chain, are soluble in $scCO_2$.[16] Copolymers with an irradiation-sensitive hydrocarbon moiety and a second fluorinated segment have been synthesized and investigated using $scCO_2$.[2,3] Block copolymers with >60 vol% fluorocomponent have been developed in $scCO_2$ at pressures >4000 psi and temperatures >40°C. Negative-tone features of 200 nm and positive-tone features of 400 nm were resolved.

In this paper, we report using iCVD copolymerization to incorporate fluorinated acrylics into irradiation-sensitive CVD thin films. The goal is to create patterns in these CVD thin films using low-dosage e-beam exposure and $scCO_2$ development. Both negative-tone and positive-tone contrast can be achieved.

5.2 Experimental Methods

Films were deposited onto silicon wafer substrates placed on a water-cooled stage (25 °C) in a custom-built 200 mm diameter reactor described elsewhere.[17] The reactor was equipped with a stainless steel filament array, which was resistively heated to 250°C to thermally decompose the initiator. Tert-butyl peroxide (Aldrich) was used as the initiator and vaporized at room temperature. Glycidyl methacrylate (GMA), methacrylic acid (MAA),

2,2,3,3,4,4,5,5,6,6,7,7-dodecafluoroheptyl acrylate (DFHA, CH_2=$CHCOOCH_2(CF_2)_5CF_2H$), and 2-(perfluoroalkyl) ethyl methacrylate (PFEMA, CH_2=$C(CH_3)COOCH_2CH_2(CF_2)_nCF_3$, n~7) were obtained from Aldrich and vaporized in glass jars that were heated to 62°C, 70°C, 75°C, and 90 °C, respectively. The flow rates of initiator and monomers were regulated using needle valves. In the copolymerization of GMA and DFHA, flow rates of peroxide and GMA were kept constant at 0.1 and 0.8 sccm, respectively, while the DFHA flow rate was varied between 0 and 0.65 sccm to synthesize copolymers with different compositions. The reactor pressure was maintained at 0.3 torr. P(MAA-PFEMA) copolymer was synthesized using a MAA flow rate of 1.2 sccm and a PFEMA flow rate of 0.2 sccm. Pressure in the reactor chamber was maintained at 0.4 torr. Annealing of the P(MAA-PFEMA) thin film was carried out in vacuum at 160°C for 60 mins.

Fourier-transform infrared (FTIR) measurements were performed on a Nicolet Nexus 870 spectrometer in normal transmission mode using a DTGS KBr detector over the range of 400-4000 cm^{-1} at 4 cm^{-1} resolution over 64 scans. Electron-beam irradiation was done using a Cambridge EBMF lithography tool with an acceleration voltage of 40 kV. Supercritical CO_2 development was performed in a supercritical fluid extraction system from Supercritical Fluid Technologies for 10 mins. SCF grade 4.0 liquid CO_2 was introduced into the processing vessel, which was heated to 35°C or 45°C, and the pressure was varied between 3000 psi and 6000 psi. An HPLC pump was used to inject 2 vol% ethanol into the fluid as the cosolvent. Film thickness was measured using profilometry (Tencor P10). Samples were examined using a Leica 440 scanning electron microscope.

5.3 Results and Discussion

P(GMA-DFHA) copolymer thin films were deposited using different mole fraction of DFMA in the feed, f_A. Figure 5-1 shows the FTIR spectra of homopolymer PDFHA (H1), homopolymer PGMA (H2), and two P(GMA-DFHA) copolymers synthesized using $f_{A=}$ 0.20 (C1) and $f_{A=}$ 0.81 (C2). The strong absorption ranging from 1150 cm^{-1} to 1220 cm^{-1} in H1 is assigned to CF_2 stretching,[17] and the small peak at 909 cm^{-1} in H2 is assigned to the absorption of the epoxy group.[18] The presence of the characteristic absorptions for CF_2 and epoxy groups in the spectra of copolymers suggests incorporation of both DFHA and GMA components through the vapor phase synthesis.

Assuming GMA and DFHA have the same C=O bond oscillator coefficient, the concentrations of epoxy and C=O groups in the as-deposited copolymer films are proportional to the peak areas of the epoxy at 909 cm^{-1} (A_{epoxy}) and the C=O ($A_{C=O}$), with the latter containing contributions from both GMA (1730 cm^{-1}) and DFHA (1760 cm^{-1}). Thus the mole fraction of DFHA in the deposited film can be calculated using equation: $F_A = 1 - \frac{A_{epoxy}}{rA_{C=O}}$, where r is the peak area ratio of epoxy and C=O absorption in homopolymer PGMA. Figure 5-2a shows the plot of the resulting F_A in the deposited material versus the DFHA feed mole fraction (f_A), demonstrating the capability of systematically tuning film composition using iCVD. Theoretically, the copolymer composition can be related to monomer gas feed mole fraction using the Fineman-Ross copolymerization equation:[19]

$$\frac{f_A(1-2F_A)}{F_A(1-f_A)} = r_B + \left[\frac{f_A^2(F_A-1)}{F_A(1-f_A)^2}\right] r_A$$

where r_A is the reactivity ratio of DFHA, and r_B is the reactivity ratio of GMA. Therefore the plot of $\frac{f_A(1-2F_A)}{F_A(1-f_A)}$ versus $\frac{f_A^2(F_A-1)}{F_A(1-f_A)^2}$ provides a method to calculate the monomer reactivity ratios, as shown in Figure 5-2b. r_A is estimated to be 0.21 from the slope of the least-squares linear regression, and r_B is estimated to be 0.15 from the intercept. Since both r_A and r_B are greater than zero and less than unity, the possibilities of alternating and block copolymerization can be excluded,[20] indicating that random P(DFHA-GMA) copolymers are produced in the iCVD synthesis process.

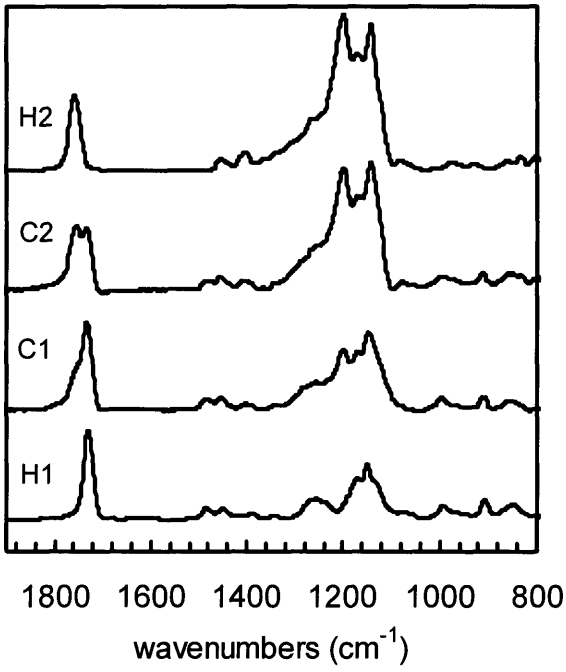

Figure 5-1. FTIR spectra of homopolymer PDFHA (H1), homopolymer PGMA (H2), copolymer P(GMA-DFHA) with DFHA gas feed ratio of 0.20 (C1) and 0.81 (C2).

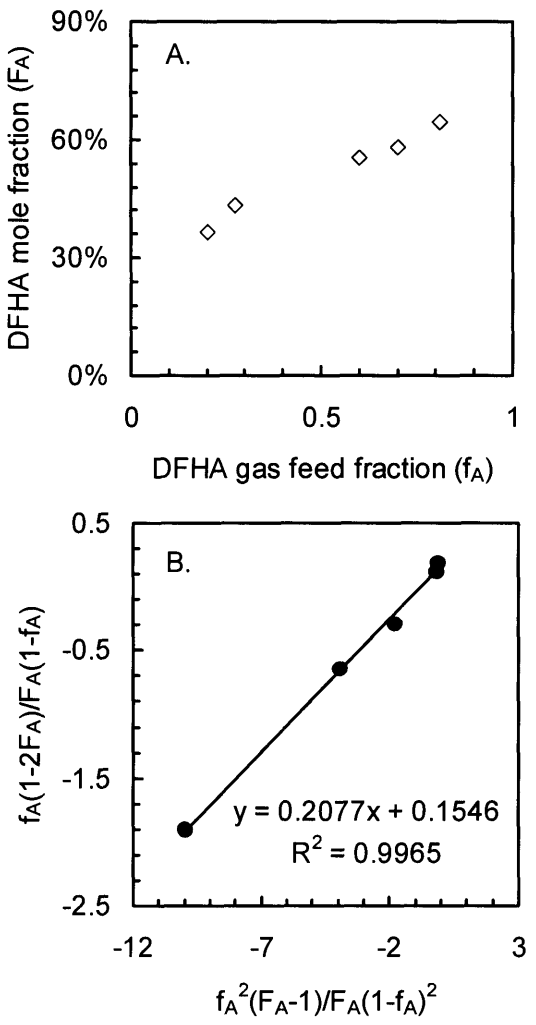

Figure 5-2. Systematic tuning of copolymer film composition during iCVD. A) relationship between DFHA mole fractions in P(GMA-DFHA) copolymers, F_A and DFHA gas feed mole fractions, f_A; and B) plot of the Fineman-Ross copolymerization equation, which gives the estimation of monomer reactivity ratios: $r_A = 0.21$, $r_B = 0.15$.

The dissolution behavior of the P(GMA-DFHA) copolymers was tested in $scCO_2$. Based on the dissolution condition of fluorinated resists reported in literature,[2] the processing time and temperature were fixed at 10 mins and 45°C, respectively, while the processing pressure was varied from 3000 psi to 6000 psi. Three competing interactions affect the $scCO_2$

solubility of the copolymer: the segment-segment interaction within the copolymer, the interaction between polar groups and $scCO_2$, and the interaction between non-polar CF_2 groups and $scCO_2$. Copolymers with higher DFHA content demonstrate higher $scCO_2$ solubility, because the CF_2-CO_2 interaction dominates and favors the dissolving of the copolymer. As the processing pressure increases, the solubility of the copolymer improves, as shown in Figure 5-3. However, the copolymer with 67 mol% DFHA still has 17% thickness remained as pressure reaches 6000 psi. This incomplete solubility is attributed to random nature of the copolymer and the CHF_2 end group in DFHA.[2]

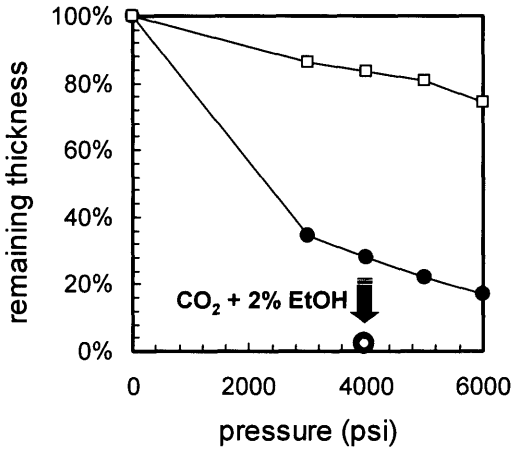

Figure 5-3. Percentage of thickness remained in P(GMA-DFHA) copolymer thin films with 35 mol% DFHA (□) and 67 mol% DFHA (●) after development in $scCO_2$ for 10 mins.

Addition of low concentrations of cosolvents into $scCO_2$ has been explored in surface cleaning and resists stripping to improve the solvating power of CO_2.[4] In general, cosolvents can increase the polarity and polarizability of the resulting fluid.[21] It was observed that the copolymer with 65 mol% DFHA became completely soluble in $scCO_2$ at 45°C, 4000 psi,

when 2 vol% of ethanol was added as a cosolvent. In addition, the copolymer films can be patterned after electron-beam exposure of 80 $\mu C/cm^2$ and subsequent $scCO_2$ development with 2 vol% of ethanol. The dosage was chosen based on previous investigation of PGMA e-beam sensitivity[14] and is much lower than the dosage required for development of CVD PTFE thin films.[9] Figure 5-4 shows 500 and 300 nm negative-tone features resolved, which are comparable to what have been achieved in spin-coated $scCO_2$ developable resists.[2,3] However, features were distorted due to the swelling of crosslinked PGMA network, a common characteristic of negative-tone resists with crosslinking mechanism.[22]

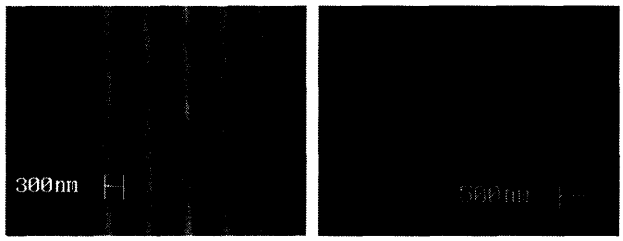

Figure 5-4. Negative-tone 300 and 500 nm features achieved in P(GMA-DFHA) copolymers after electron-beam exposure and $scCO_2$ development with 2 vol% ethanol added as a cosolvent.

In order to overcome the swelling problem, an imaging material not requiring crosslinking chemistry needs to be explored. P(MAA-PFEMA) copolymers were synthesized using iCVD. The carboxylic acid in the MAA component can form an anhydride through dehydration reaction in 160°C annealing.[23] The resulting anhydride functionality is highly electron-withdrawing and enhances the propensity of polymer chain breaking under e-beam irradiation,[24] creating a positive-tone contrast through a non-crosslinking chemistry. The PFEMA component bears a CF_3 end group and is expected to further improve $scCO_2$

solubility over DFHA.[25]

Figure 5-5 shows the FTIR spectrum of an iCVD P(MAA-PFEMA) copolymer synthesized using a PFEMA gas feed ratio of 0.14. The carbonyl absorption appears as a doublet, with the 1740 cm^{-1} peak assigned to C=O stretching in PFEMA, and the 1702 cm^{-1} peak assigned to C=O stretching in MAA.[23] The CF_2 stretching[17] at 1150 and 1210 cm^{-1} and the CF_3 stretching[26] at 1240 cm^{-1} are clearly resolved. The PFEMA composition was calculated to be 30 mol% using the fitting method in the C=O stretching region.[23,27] Figure 5-6 shows 300 nm resolution achieved after an e-beam irradiation of 100 $\mu C/cm^2$ followed by pure $scCO_2$ development at 35°C and 3000 psi. Compared with DFHA copolymers, the ability to develop post-annealed PFEMA copolymers with lower content of fluorine-containing component at milder condition is attributed to the contribution of the CF_3 end group to the $scCO_2$ solubility. The non-swelling nature of the features indicates the potential of producing high-quality patterns using this positive-tone CVD imaging material.

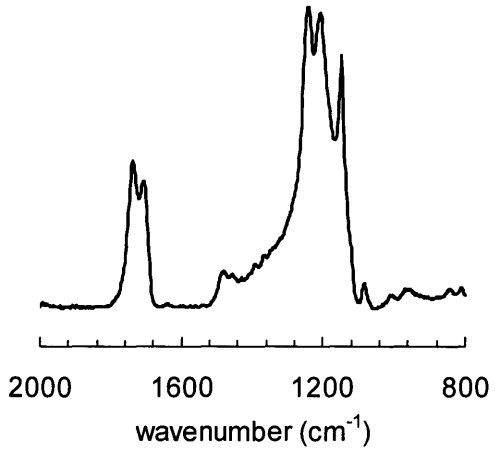

Figure 5-5. FTIR spectrum of P(MAA-PFEMA) copolymer synthesized by iCVD.

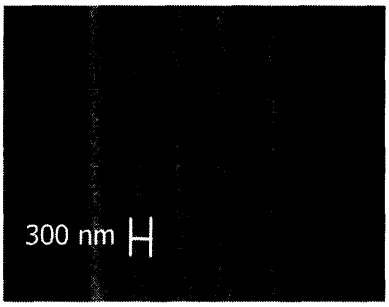

Figure 5-6. Resolution achieved in a post-annealed PFEMA copolymer using e-beam exposure followed by pure $scCO_2$ development at 35°C and 3000 psi.

5.4 Conclusions

P(GMA-DFHA) and P(MAA-PFEMA) copolymers were synthesized using iCVD. The incorporation of fluorinated acrylics changes hydrocarbon polymers that are poorly soluble in $scCO_2$ to CO_2-processable copolymers. The crosslinking chemistry of epoxy groups in P(GMA-DFHA) thin films creates a negative-tone contrast after e-beam exposure, and 300 nm features were obtained using $scCO_2$ development with 2 vol% ethanol added as a cosolvent. The chain scission in post-annealed P(MAA-PFEMA) thin films forms 300 nm non-swelling positive-tone images. The CF_3 end groups in PFEMA contribute to higher $scCO_2$ solubility than DFHA, allowing development of PFEMA copolymers with lower content of fluorine-containing component at milder condition than DFHA copolymers. These results are comparable to the development of $scCO_2$ resists produced by spin coating. The ongoing work includes further understanding of process limits and improvement of the resolution.

5.5 References

(1) Allen, R. D.; Chen Rex, K. J.; Gallagher-Wetmore, P. M. *Proceedings of SPIE: The International Society for Optical Engineering*, 1995, *2438*, 250.

(2) Sundararajan, N.; Yang, S.; Ogino, K.; Valiyaveettil, S.; Wang, J. G.; Zhou, X. Y.; Ober, C. K.; Obendorf, S. K.; Allen, R. D. *Chem. Mat.* **2000,** *12*, 41.

(3) Pham, V. Q.; Ferris, R. J.; Hamad, A.; Ober, C. K. *Chem. Mat.* **2003,** *15*, 4893.

(4) Weibel, G. L.; Ober, C. K. *Microelectron. Eng.* **2003,** *65*, 145.

(5) Goldfarb, D. L.; de Pablo, J. J.; Nealey, P. F.; Simons, J. P.; Moreau, W. M.; Angelopoulos, M. *J. Vac. Sci. Technol. B* **2000,** *18*, 3313.

(6) Horn, M. W.; Pang, S. W.; Rothschild, M. *J. Vac. Sci. Technol. B* **1990,** *8*, 1493.

(7) Horn, M. W.; Rothschild, M.; Maxwell, B. E.; Goodman, R. B.; Kunz, R. R.; Eriksen, L. M. *Appl. Phys. Lett.* **1996,** *68*, 179.

(8) Nalamasu, O.; Wallow, T. I.; Reichmanis, E.; Novembre, A. E.; Houlihan, F. M.; Dabbagh, G.; Mixon, D. A.; Hutton, R. S.; Timko, A. G.; Wood, O. R.; Cirelli, R. A. *Microelectron. Eng.* **1997,** *35*, 133.

(9) Lewis, H. G. P.; Weibel, G. L.; Ober, C. K.; Gleason, K. K. *Chem. Vapor Depos.* **2001,** *7*, 195.

(10) Medeiros, D. R.; Aviram, A.; Guarnieri, C. R.; Huang, W. S.; Kwong, R.; Magg, C. K.; Mahorowala, A. P.; Moreau, W. M.; Petrillo, K. E.; Angelopoulos, M. *IBM J. Res. Dev.* **2001,** *45*, 639.

(11) Ito, H.; Ueda, M. *Macromolecules* **1988,** *21*, 1475.

(12) Mao, Y.; Gleason, K. K. *Langmuir* **2004,** *20*, 2484.

(13) Mao, Y.; Gleason, K. K. submitted to *Langmuir*.

(14) Mao, Y.; Felix, N. M.; Nguyen, P. T.; Ober, C. K.; Gleason, K. K. *J. Vac. Sci. Technol. B* **2004,** *22*, 2473.

(15) McHugh, M. A.; Krukonis, V. J. *Supercritical Fluids Extraction: Principles and Practice*. 2nd ed.; Butterworth-Heineman: Stoneham, MA, 1993.

(16) Desimone, J. M.; Maury, E. E.; Menceloglu, Y. Z.; McClain, J. B.; Romack, T. J.; Combes, J. R. *Science* **1994,** *265*, 356.

(17) Lau, K. K. S.; Murthy, S. K.; Lewis, H. G. P.; Caulfield, J. A.; Gleason, K. K. *J. Fluor.*

Chem. **2003,** *122*, 93.

(18) Hwang, N. M.; Cheong, W. S.; Yoon, D. Y.; Kim, D. Y. *J. Cryst. Growth* **2000,** *218*, 33.

(19) Fineman, M.; Ross, S. D. **1950,** *5*, 259.

(20) Odian, G. *Principles of Polymerization.* 2nd ed.; Wiley-Interscience: New York, 1981.

(21) Ekart, M. P.; Bennett, K. L.; Ekart, S. M.; Gurdial, G. S.; Liotta, C. L.; Eckert, C. A. *Aiche J.* **1993,** *39*, 235.

(22) Thompson, L. F.; Willson, C. G. *Introduction to Microlithography.* 2nd ed.; American Chemical Society: Washington, DC, 1994.

(23) Lee, J. Y.; Painter, P. C.; Coleman, M. M. *Macromolecules* **1988,** *21*, 346.

(24) Moreau, W.; Merritt, D.; Moyer, W.; Hatzakis, M.; Johnson, D.; Pederson, L. **1979,** *16*, 1989.

(25) Dardin, A.; DeSimone, J. M.; Samulski, E. T. *J. Phys. Chem. B* **1998,** *102*, 1775.

(26) Labelle, C. B.; Gleason, K. K. *J. Electrochem. Soc.* **2000,** *147*, 678.

(27) Dong, J.; Tsubahara, N.; Fujimoto, Y.; Ozaki, Y.; Nakashima, K. *Appl. Spectrosc.* **2001,** *55*, 1603.

CHAPTER SIX

Vapor Deposited Fluorinated Glycidyl Copolymer Thin Films with Low Surface Energy and Improved Mechanical Properties

Y. Mao, K. K. Gleason.

Abstract

Initiated chemical vapor deposition (iCVD) copolymers of glycidyl methacrylate (GMA) with two fluorinated acrylics, 2,2,3,3,4,4,5,5,6,6,7,7-dodecafluoroheptyl acrylate (DFHA) and 2-(perfluoroalkyl) ethyl methacrylate (PFEMA) were investigated to demonstrate how to achieve high mechanical properties and optical transparency while retaining low surface energies. The self-crosslinking of the GMA component upon annealing provides improvement of mechanical properties. The ratio of the fluorinated acrylics to GMA was intentionally varied through iCVD to provide systematic control over the copolymer surface and bulk mechanical properties. The hardness of the post-annealed DFHA and PFEMA iCVD copolymers is an order of magnitude higher than their corresponding homopolymers, and their dispersive surface energy is in the range of 9.9-18.6 mN/m. The surface segregation of fluorine contributes to the low surface energy of iCVD fluorinated copolymers with low fluorine content. Transmission greater than 99% across the visible spectrum has been achieved in these iCVD fluorinated copolymers.

Acknowledgements

We gratefully acknowledge the support of the NSF/SRC Engineering Research Center for Environmentally Benign Semiconductor Manufacturing. This work made use of MRSEC Shared Facilities supported by the National Science Foundation under Award Number DMR-9400334. We also thank Dr. Qingguo Wu for help in nanoindentation experiments.

6.1 Introduction

Low surface energy finishes that are mechanically durable and optically transparent are desirable in many applications such as non-wettable, non-stick, and anti-fouling coatings.[1-4] Poly(tetrafluoroethylene) (PTFE, $(-CF_2-)_n$) may be considered as the benchmark for low surface energy coatings ($\gamma_s \sim 20$ mN/m).[5] Acrylic polymers with long fluorinated side chains exhibit lower values of γ_s due to their comb-like structure and CF_3 endgroups.[6,7] However, the mechanical properties of these fluoropolymer coatings are poor, because the weak intermolecular forces between fluorinated chains limit the cohesion in the coatings: for example, the hardness of PTFE is about 0.06 GPa,[8] while most traditional polymers exhibit hardness ~0.2 GPa.[9] The softness of coatings results in poor abrasion resistance and limits the applications of fluoropolymer coatings. Crosslinkers have been added to achieve desired mechanical properties in fluoropolymers coatings,[2,10] but fundamental understanding of the tradeoff between increase of mechanical properties and degradation of surface properties is needed, since most crosslinkers usually bear polar groups and introduce increase of surface energy. Additionally, the crystallinity of homopolymer PTFE reduces its transparency, and the high level of fluorine in fluoropolymers may introduce haze due to the phase segregation of fluorinated domains, making amorphous fluorinated copolymers with lower fluorine content desirable for applications requiring optical clarity.

In this work, copolymers of fluorinated acrylics and glycidyl methacrylate (GMA) will be synthesized using initiated chemical vapor deposition (iCVD). The epoxy rings in GMA component can self-crosslink upon annealing,[11] allowing improvement of mechanical properties. The ratio of the fluorinated acrylics to GMA will be intentionally varied through iCVD, in order to provide systematic control over the copolymer surface and bulk

mechanical properties. The goal is to improve mechanical properties of fluorinated acrylic thin films without sacrificing their desirable surface properties.

There are many advantages of using the dry process of chemical vapor deposition (CVD) to produce low surface energy thin films. The CVD method provides uniform coverage over large areas, low roughness, and conformal coatings.[12] CVD can produce thin films on soluble substrates and thus can be extended to a wide range of new material applications.[13] Additionally, CVD can coat nanoscale features[14] as well as substrates with complex geometries. From the perspective of thin film processing, CVD serves as a promising method to avoid the harsh conditions in traditional low surface energy coatings synthesis, since PTFE and fluorinated acrylic polymers generally require sintering conditions or special solvents to create the final coatings.[6,7] Plasma CVD is a common method for preparing polymeric thin films. It has been reported to produce crosslinked hydrophobic fluorinated acrylic thin films with functionalities retained through pulsing of the plasma discharge.[15]

iCVD provides a complementary method to plasma CVD for depositing low surface energy thin films with systematic control of film structure. iCVD is a one-step synthesis technique involving thermal decomposition of initiators and subsequent addition reaction of monomer species.[16,17] Using tert-butyl peroxide (TBP) as the initiator, iCVD has been successfully applied in producing poly(glycidyl methacrylate) thin films with full retention of epoxy groups.[16] The weak peroxide bond in TBP allows use of very low filament temperatures (180–250°C) to generate radicals, which initialize chain reaction of monomers. The low temperatures limits the bond-scission chemistry to the fragmentation of TBP, while retain the pendant epoxy groups of the gaseous monomer.

In this paper, we report the iCVD copolymerization of GMA with two fluorinated acrylics, 2,2,3,3,4,4,5,5,6,6,7,7-dodecafluoroheptyl acrylate (DFHA, CH_2=$CHCOOCH_2(CF_2)_5CF_2H$) and 2-(perfluoroalkyl) ethyl methacrylate (PFEMA, CH_2=$C(CH_3)COOCH_2CH_2(CF_2)_nCF_3$, n~7). The copolymer thin films were annealed to introduce crosslinks. These resulting thin films were characterized by contact angle analysis, infrared spectroscopy, and nanoindentation. The systematic study of post-annealed fluorinated glycidyl copolymer thin films demonstrates how to achieve superior mechanical properties while retaining low surface energies.

6.2 Experimental Methods

Films were deposited onto silicon wafer or glass slide substrates in a custom-built reactor. The reactor was equipped with a stainless steel filament array, which was resistively heated to 220°C-250°C to thermally decompose the initiator, and a water-cooled stage (35 °C) on which the substrate was placed. Pressure in the vacuum chamber was maintained at 0.3-0.5 torr. GMA, DFHA, and PFEMA were obtained from Aldrich and vaporized in glass jars that were heated to 62°C, 75 °C, and 90 °C, respectively. Tert-butyl peroxide (Aldrich) was used as the initiator and vaporized at room temperature. The flow rates of peroxide and GMA were regulated using needle valves and kept constant at 0.1 and 0.8 sccm, while the flow rates of DFHA and PFEMA were varied between 0 and 1 sccm to synthesize copolymers with different compositions. Other experimental set-up details have been described previously.[18,19]

Fourier transform infrared (FTIR) measurements were done on a Nicolet Nexus 870 spectrometer in normal transmission mode using a DTGS KBr detector over the range of

400-4000 cm^{-1} at 4 cm^{-1} resolution. Angle-resolved X-ray photoelectron spectroscopy (ADXPS) was performed on a Kratos Axis Ultra spectrometer using a monochromatized aluminum K α source at take-off angles of 20, 55, and 90°. Dynamic contact angle measurements were performed on a goniometer equipped with an automatic dispenser (Ramé-Hart). Water and a series of linear alkanes (hexane, heptane, octane, decane, dodecane, and hexadecane) were used as test liquids. The transmission of copolymer thin films was measured using a FluoroMax-2 UV-Vis spectrometer within the wavelength range of 400-800 nm.

Measurements of hardness and elastic modulus were performed using a Nano Indenter XP (Nano Instruments) and MTS continuous stiffness measurement technique. A Berkovick diamond tip was used in the measurements. Film thicknesses of >1 μm were used to minimize any substrate effects. Measurements at ten points were taken for each sample. It is generally accepted that the substrate impact is minimal at penetration depths of less than 10% of the film thickness.[20,21] Therefore, following standard protocol, the hardness is reported at 10% of the film thickness and the modulus is taken at 50 nm. Film thickness was measured using variable-angle spectroscopic ellipsometry (VASE) with the Cauchy-Urbach model used for data fitting. Film surface roughness was measured using atomic force microscopy performed on a Digital Instruments Dimension 3000 under tapping mode.

6.3 Results and Discussion

In order to investigate the effect of copolymer composition on material properties, we deposited P(GMA-DFHA) copolymer thin films with different DFHA contents by adjusting the gas feed fractions of monomer GMA and DFHA. This has been proven as an effective

way to systematically control the composition in iCVD copolymers.[22] Figure 6-1 shows the FTIR spectra of homopolymer PDFHA (H1), homopolymer PGMA (H2), and copolymer P(GMA-DFHA) as-deposited using DFHA feed fraction of 0.28 (C) and after vacuum annealing at 200°C for 14 hrs (C′). The annealing temperature was chosen to avoid thermal decomposition of ester side groups in acrylic copolymers.[23] The strong absorption ranging from 1150 cm^{-1} to 1220 cm^{-1} in H1 is assigned to CF_2 stretching,[19] and the small peak at 909 cm^{-1} in H2 is the characteristic absorption peak of the epoxy group.[24] The spectrum of copolymer C displays this characteristic epoxy absorption, indicating incorporation of GMA component into the PDFHA chain through iCVD copolymerization. The disappearance of the 909 cm^{-1} absorption peak in C′ suggests the occurrence of epoxy ring-opening crosslinking reaction, which is further confirmed by the insolubility of thin films in common solvents for polymethacrylates such as tetrahydrofuran.

Based on the Beer-Lambert equation[25] and the assumption that the C=O bond oscillator coefficient is the same in GMA and DFHA, the concentrations of epoxy and C=O groups in the as-deposited copolymer films are proportional to the peak areas of the epoxy at 909 cm^{-1} (A_{epoxy}) and the C=O ($A_{C=O}$), with the latter containing contributions from both GMA (1730 cm^{-1}) and DFHA (1760 cm^{-1}). Thus the DFHA mole fraction can be calculated using equation: $f_{DFHA} = 1 - \frac{A_{epoxy}}{rA_{C=O}}$, where r is the peak area ratio of epoxy and C=O absorption in homopolymer PGMA. Using this approach, the compositions of copolymers deposited using DFHA flow ratio of 0.12, 0.28, and 0.81 were analyzed to have 27%, 45%, and 65% DFHA, respectively. Similarly, the reaction extent of epoxy groups, X, in annealing copolymer samples can be calculated from the epoxy absorption peak area after annealing

(A'_{epoxy}) and before annealing (A_{epoxy}): $X = 1 - \frac{A'_{epoxy}}{A_{epoxy}}$. As shown in Fig. 6-2, P(GMA-DFHA) copolymers with different compositions demonstrate similar crosslinking reaction trends with time. More than 90% of epoxy groups have reacted after annealing 6 hrs, and complete crosslink reaction of epoxy groups was achieved in 14 hrs.

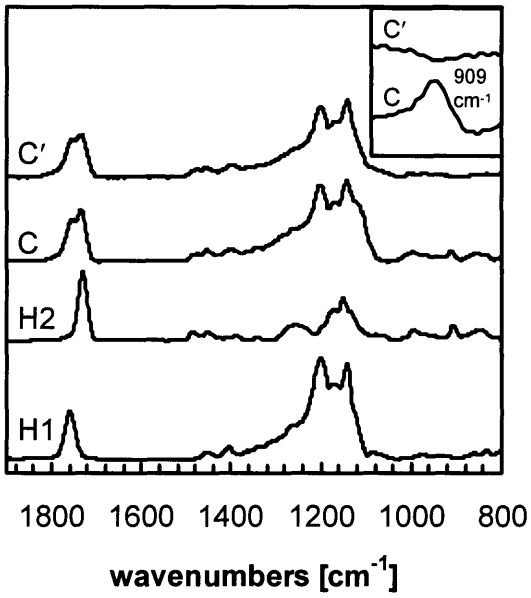

Figure 6-1. FTIR spectra of homopolymer PDFHA (H1), homopolymer PGMA (H2), copolymer P(GMA-DFHA) as-deposited with DFHA gas flow ratio 0.28 (C) and after 14 hrs annealing (C′).

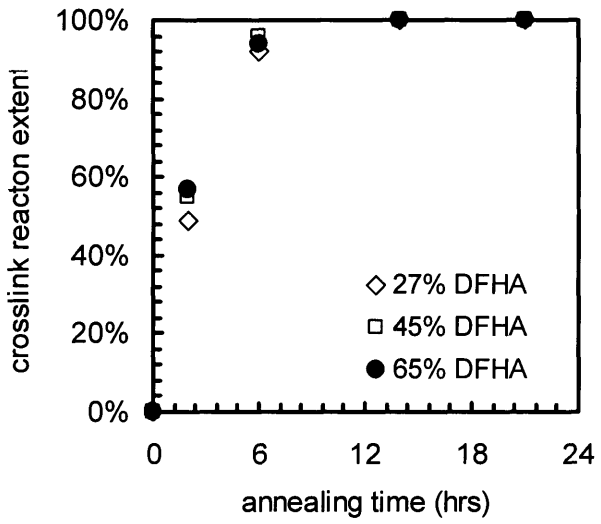

Figure 6-2. Crosslinking extent of epoxy groups in P(GMA-DFHA) copolymers calculated from the absorption intensity change in epoxy peak at 909 cm^{-1}.

Figure 6-3 shows the mechanical property changes of P(GMA-DFHA) copolymer thin films after annealing. Both the hardness and modulus of the films improve significantly. For example, the hardness of copolymer with 27% DFHA increases from 0.06 GPa to 0.36 GPa after annealing 6 hrs, and its modulus increases from 1.3 GPa to 5.8 GPa. The slower rate of improvement in mechanical properties after annealing 6 hrs is probably due to the near completion of epoxy crosslinking reaction, as indicated in Figure 6-2. The slight decrease of hardness and modulus after 21 hrs of annealing is attributed the onset of film decomposition, which can be inferred from the broadening of the C=O absorption peak in the FTIR spectra (not shown).

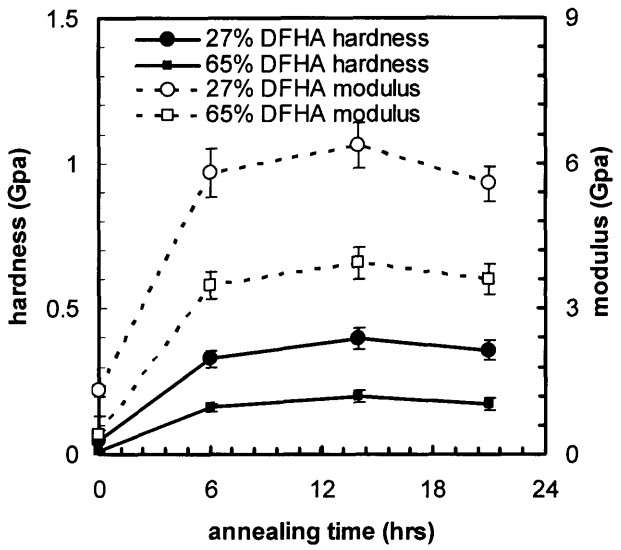

Figure 6-3. Mechanical property improvement of P(GMA-DFHA) copolymer thin films after annealing. In comparison, the hardness of PTFE coatings is ~0.06 GPa, and the modulus is 2.3 GPa.[8]

P(GMA-PFEMA) copolymer thin films with different PFEMA compositions were also synthesized using iCVD and analyzed using the FTIR method as discussed for the P(GMA-DFHA) copolymers. Table 6-1 lists contact angles of three different solvents on P(GMA-DFHA) and P(GMA-PFEMA) copolymer thin films annealed for 14 hrs. Compared to P(GMA-DFHA) with CF_2H terminated side chains, P(GMA-PFEMA) with CF_3 terminated side chains demonstrates much higher hydrophobicity. Indeed, the advancing contact angle (θ_{ad}) is greater than 120° for water for all three PFEMA copolymer films. It is expected that the fluorinated segments have low surface energy and will segregate to the air-polymer interface, which is suggested from the high values of contact angles resulting with small amount of PFEMA incorporation.[10] With increasing fluorine content, the contact angle of water and other dispersive liquids on P(GMA-PFEMA) increases, indicating decrease in

wettability. It is noteworthy that these thin films exhibit extremely small root mean square roughness, 0.3-0.8 nm. The smoothness of these films precludes the cause of hydrophobicity due to surface roughness.[3,26] Therefore the data represent the intrinsic wettability of the thin films that is associated with the molecular structure.

Table 6-1. Contact angles of three different solvents on P(GMA-DFHA) and P(GMA-PFEMA) copolymer thin films after 14 hrs annealing.

Solvent	Advancing angle (deg)	Receding angle (deg)	Stationary angle (deg)
27% DFHA			
Octane	29.0	27.6	28.5
Hexadecane	49.6	48.0	49.1
Water	97.7	76.6	91.8
40% DFHA			
Octane	31.0	28.6	30.2
Hexadecane	50.9	49.2	50.6
Water	99.6	77.1	95.4
65% DFHA			
Octane	35.2	33.8	34.7
Hexadecane	52.8	51.2	52.3
Water	102.2	78.9	98.6
19% PFEMA			
Octane	47.9	46	47.5
Hexadecane	62.5	60.1	62.1
Water	120.2	78.9	98.6
48% PFEMA			
Octane	60.2	58.0	59.5
Hexadecane	73.7	72.0	73.5
Water	123.6	88.7	115.3
65% PFEMA			
Octane	65.0	63.1	64.8
Hexadecane	79.6	77.4	79.0
Water	126.9	90.3	118.8

Table 6-2. Dispersive surface energy (γ_d) and Zisman critical surface energy (γ_c) of post-annealed P(GMA-DFHA) and P(GMA-PFEMA) copolymer thin films.

	annealed 6 hrs		annealed 14 hrs	
composition	γ_c (mN/m)	γ_d (mN/m)	γ_c (mN/m)	γ_d (mN/m)
27% DFHA	19.2	20.3	18.4	18.6
40% DFHA	18.9	19.5	17.8	18.2
65% DFHA	17.9	18.1	16.7	17.5
19% PFEMA	13.3	15.2	12.5	14.7
48% PFEMA	12.4	12.6	11.2	11.8
65% PFEMA	10.8	11.6	9.6	9.9

Measurement of surface energy is not straightforward, and methods based on contact angle are usually used for practical reasons.[5,10,15] The Zisman plot was widely applied to determine the critical surface tension of a surface, γ_c, by plotting contact angles (θ) of non-polar liquids versus their surface tensions (γ_l) and extrapolating γ_l to $\cos\theta = 1$.[27] It must be noted that there is no theoretical justification for equating γ_c with the surface energy of a material. An alternative is to calculate the dispersion force component of the surface energy, γ_d, using the Good-Girifalco-Fowkes equation,[23,24] which has the form of $\cos\theta = -1 + 2(\gamma_s^d / \gamma_l)^{1/2}$ and has been theoretically justified.[3] For purpose of systematic comparison, Table 6-2 gives the Zisman critical surface tension and dispersive surface energy for P(GMA-DFHA) and P(GMA-PFEMA) copolymers annealed for 6 and 14 hrs. PFEMA copolymers, with CF_3 pendant end groups, demonstrate much lower surface energies than DFHA copolymers, with CF_2H pendant end groups. The surface energies of copolymers annealed for 14 hrs is lower compared to those annealed for 6 hrs. This

improvement can be attributed to a higher degree of immobilization of fluoroalkyl groups after a longer annealing time.[28]

Table 6-3. Fluorine surface segregation data of P(GMA-PFEMA) copolymer thin films after annealing 14 hrs.

PFEMA content	F/C atomic ratio		XPS sampling depth (nm)
	FTIR	XPS	
48%	0.65	1.40	2.7
		1.24	6.6
		1.20	8
65%	0.79	1.54	2.7
		1.37	6.6
		1.35	8

ADXPS was used to quantify the fluorine to carbon (F/C) atomic ratios as a function of sampling depth for P(GMA-PFEMA) copolymers after 14 hrs annealing. The results are shown in Table 6-3. Sampling depth (depth = $3\lambda \sin \alpha$) were calculated based on the take-off angle (α) and the photoelectron escape depth (λ) estimated by Schmidt et al.[2] The bulk F/C atomic ratios were calculated from the mole fractions of fluorinated acrylics obtained from the FTIR composition analysis. The F/C ratios in the first 8 nm of the surface are much higher than the bulk F/C ratios, and the F/C ratios decrease as the sampling depth increases, indicating that the perfluorinated segments segregate to the air-polymer interface. No minimum F/C ratios were observed in the first 8 nm of the surface. When surfaces become enriched in fluorine, a fluorine-depleted subsurface region can be observed.[2] However, continuous decrease of fluorine concentration below the surface was also seen in fluorinated copolymer coatings.[10,29] The iCVD polymers show a similar lack of fluorine-depleted region. The surface enrichment of fluorine content explains the low surface energies of copolymers

with 48% PFEMA (γ_d =11.8 mN/m) and 65% PFEMA (γ_d =9.9 mN/m). Indeed, the high F/C ratios and the small surface energies suggest rather closely packed perfluorinated segments at the surface.[5]

Figure 6-4 summarizes the mechanical properties and surface energies for iCVD P(GMA-DFHA) and P(GMA-PFEMA) copolymers after annealing 14 hrs. With an equal amount of fluorine-containing monomer, P(GMA-PFEMA) copolymers show slightly lower mechanical properties than P(GMA-DFHA) copolymers, possibly due to smaller cohesion forces between perfluorinated chains compared with the $-(CF_2)_n-CF_2H$ chains. These two copolymers behave similarly in terms of mechanical property change with surface energy: the lower the surface energy, the smaller the hardness and modulus of thin films after annealing due to the higher fluorine content. The dispersive surface energies of DFHA and PFEMA copolymers are slightly higher than the γ_d of their corresponding homopolymers. However, the annealed copolymers demonstrate more than 10 times improvement in hardness, and their moduli increase more than 4 times. Compared with PTFE coatings, annealed DFHA and PFEMA copolymers exhibit superior mechanical properties, yet retain low dispersive surface energies.

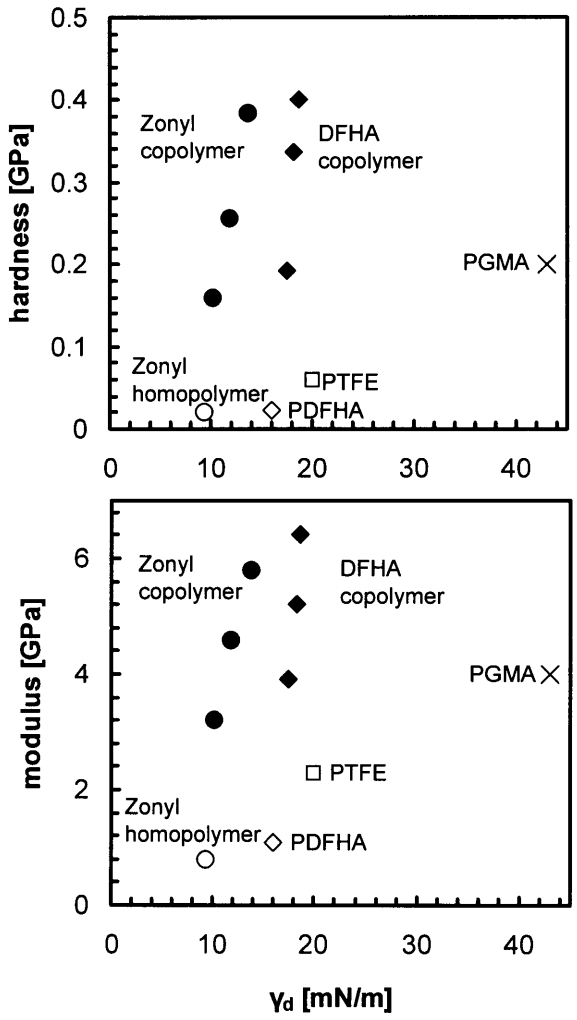

Figure 6-4. Mechanical properties and dispersive surface energies of PFEMA copolymers (●) and DFHA copolymers (♦) after annealing 14 hrs compared with PFEMA homopolymer (○), DFHA homopolymer (◊), PTFE(□),[5,8] and unannealed PGMA (×). Annealed DFHA and PFEMA copolymers demonstrate enhancement in both mechanical properties and surface properties compared with PTFE coatings.

The iCVD copolymer thin films exhibit excellent transparency within the visible wavelength range. The transmission of all the P(GMA-DFHA) copolymer thin films (DFHA 27, 45, and 65%, thickness ~ 700 nm) is greater than 99.9% over the wavelength region 400-

800 nm. The transmission of PFEMA copolymer thin films is slightly lower than the DFHA copolymers, because perfluorinated chains are more likely to form separate domains from the hydrocarbon portion of the polymer, and the phase separation results in slight haze in the final thin films. Nevertheless, P(GMA-PFEMA) copolymers (thickness ~ 700 nm) with 19% and 48% PFEMA exhibit more than 99% transmission across the entire visible spectrum (400-800 nm) after annealing 14 hrs, a value significantly higher than what have been reported in the literature.[4]

6.4 Conclusions

Copolymer thin films that satisfy the criteria of low surface energy, high hardness and modulus, and high transmission of visible light have been prepared through an iCVD process. Post-annealed iCVD DFHA and PFEMA copolymers exhibit superior mechanical properties and lower surface energies than PTFE coating. The hardness of the post-annealed DFHA and PFEMA copolymer coatings enhances an order of magnitude compared with uncrosslinked fluoropolymers, and their dispersive surface energy is in the range of 9.9-18.6 mN/m. The surface segregation of fluorine in iCVD PFEMA copolymers contributes to the low surface energy even the fluorine content is low. In addition, these copolymer coatings exhibit > 99% transmission in the visible wavelength range. The solvent-free nature of this thin film fabrication technique creates the opportunity to apply low surface energy coatings with desirable mechanical properties and optical clarity to a wide range of substrates.

6.5 References

(1) Lindner, E. **1992,** *6*, 193.

(2) Schmidt, D. L.; Coburn, C. E.; Dekoven, B. M.; Potter, G. E.; Meyers, G. F.; Fischer, D. A. *Nature* **1994,** *368*, 39.

(3) Hozumi, A.; Takai, O. **1997,** *303*, 222.

(4) Nakajima, A. *J. Ceram. Soc. Jpn.* **2004,** *112*, 533.

(5) Thunemann, A. F.; Lieske, A.; Paulke, B. R. *Adv. Mater.* **1999,** *11*, 321.

(6) Anton, D. *Adv. Mater.* **1998,** *10*, 1197.

(7) Tsibouklis, J.; Nevell, T. G. *Adv. Mater.* **2003,** *15*, 647.

(8) Wang, J.; Shi, F. G.; Nieh, T. G.; Zhao, B.; Brongo, M. R.; Qu, S.; Rosenmayer, T. *Scr. Mater.* **2000,** *42*, 687.

(9) Briscoe, B. J.; Fiori, L.; Pelillo, E. *J. Phys. D-Appl. Phys.* **1998,** *31*, 2395.

(10) Thomas, R. R.; Anton, D. R.; Graham, W. F.; Darmon, M. J.; Sauer, B. B.; Stika, K. M.; Swartzfager, D. G. *Macromolecules* **1997,** *30*, 2883.

(11) Thompson, L. F.; Willson, C. G. *Introduction to Microlithography*. 2nd ed.; American Chemical Society: Washington, DC, 1994.

(12) Pierson, H. O. *Handbook of Chemical Vapor Deposition*. 2nd ed.; Noyes Publications: Norwich, NY, 1999.

(13) Forrest, S. R. *Nature* **2004,** *428*, 911.

(14) Lau, K. K. S.; Bico, J.; Teo, K. B. K.; Chhowalla, M.; Amaratunga, G. A. J.; Milne, W. I.; McKinley, G. H.; Gleason, K. K. *Nano Lett.* **2003,** *3*, 1701.

(15) Coulson, S. R.; Woodward, I. S.; Badyal, J. P. S.; Brewer, S. A.; Willis, C. *Chem. Mat.* **2000,** *12*, 2031.

(16) Mao, Y.; Gleason, K. K. *Langmuir* **2004,** *20*, 2484.

(17) Lewis, H. G. P.; Caulfield, J. A.; Gleason, K. K. *Langmuir* **2001,** *17*, 7652.

(18) Mao, Y.; Felix, N. M.; Nguyen, P. T.; Ober, C. K.; Gleason, K. K. *J. Vac. Sci. Technol. B* **2004,** *22*, 2473.

(19) Lau, K. K. S.; Murthy, S. K.; Lewis, H. G. P.; Caulfield, J. A.; Gleason, K. K. *J. Fluor. Chem.* **2003,** *122*, 93.

(20) Oliver, W. C.; Pharr, G. M. **1992,** *7*, 1564.

(21) Huang, X. Q.; Pelegri, A. A. *J. Eng. Mater. Technol.-Trans. ASME* **2003,** *125*, 361.

(22) Mao, Y.; Gleason, K. K. submitted to *Langmuir*.

(23) Ito, H.; Ueda, M. *Macromolecules* **1988,** *21*, 1475.

(24) Hwang, N. M.; Cheong, W. S.; Yoon, K. D.; al., e. **2000,** *218*, 33.

(25) Lin-Vien, D.; Colthup, N. B.; Fateley, W. G.; Grasselli, J. G. *The Handbook of Infrared and Raman Characteristic Frequencies of Organic Molecules*. ed.; Academic Press: San Diego, CA, 1991.

(26) Wenzel, R. N. **1949,** *53*, 1466.

(27) Zisman, W. A. **1963,** *55*, 18.

(28) Yasuda, T.; Okuno, T.; Yasuda, H. *Langmuir* **1994,** *10*, 2435.

(29) Hunt, M. O.; Belu, A. M.; Linton, R. W.; Desimone, J. M. *Macromolecules* **1993,** *26*, 4854.

CHAPTER SEVEN

Conclusions and Future Directions

7.1 Conclusions

This thesis presents a novel low-energy iCVD method for vapor-phase synthesis of functional thin films from vinyl monomers. It introduces a new peroxide initiator chemistry into the vapor deposition process, which allows selective thermal energy input into the decomposition of peroxide bonds, yet retains delicate functionalities of gaseous monomer. The introduction of initiator also enables film deposition at low filament temperature (<200°C) and greatly improves deposition rate. As a non-damaging process, the iCVD process is advantageous over conventional CVD in its capability to avoid crosslinking and retain pendant functionalities. Linear polymeric structure and full retention of epoxy functionality was achieved in iCVD PGMA thin films, as confirmed by FTIR, NMR, and X-ray photoelectron spectroscopy. Film molecular weight can be systematically varied by adjusting filament temperature and the flow ratio of initiator to monomer.

It is proposed that the iCVD process proceeds via a free radical polymerization mechanism: initiation, propagation, and termination. Study of reaction kinetics demonstrates a quantitative match of apparent activation energies with that of solution chemistry, which provides guide for extension of iCVD synthesis to other free radical vinyl polymerization systems. Polyacrylics with side groups such as carboxylic acid, chlorine, and fluorocarbon have been successfully synthesized using iCVD.

Another important accomplishment of this thesis is the iCVD synthesis of copolymers, which allows a variety of chemistry to be created and provides an approach to further tune film composition and property. The composition of copolymers can be systematically controlled by adjusting monomer flow ratios during iCVD. The analysis of iCVD

copolymerization reactivity ratios and the effect of surface temperature on copolymer molecular weights indicate that polymerization proceeds with a surface propagation mechanism. The iCVD copolymerization reactivity ratios also provide prediction of copolymer compositions.

This thesis also presents several important applications of iCVD functional thin films. The iCVD PGMA films were investigated as a negative-tone electron-beam imaging material and demonstrated sensitivity as high as 27 $\mu C/cm^2$ using conventional wet development. The P(MCA-MAA) copolymer thin films have highly electron-withdrawing anhydride functionalities incorporated after annealing, which enhances chain scission susceptibility and creates a positive-tone contrast, eliminating the typical swelling problem in negative-tone resists. The capability of using iCVD to retain delicate resist chemistry and to achieve a linear structure enables much higher resolution to be obtained than previous CVD resists. Features as small as 60 nm have been resolved. Sensitivity and resolution can be optimized through control of film molecular weight and composition in iCVD polymers. The results indicate the potential of applying this class of iCVD polymers as dry resists.

iCVD copolymerization of fluorinated acrylics with other functional monomers provides a method to create low-surface-energy coatings for specific applications. Annealed fluorinated GMA copolymers exhibit an order of magnitude improvement in mechanical properties resulting from the contribution of epoxy crosslinking in bulk upon annealing, yet their surface energy is not increased to any large extent compared with the fluorinated homopolymers due to the segregation of fluorocarbon side groups on the copolymer thin film surface.

The incorporation of fluorinated acrylics also presents the opportunity to change

hydrocarbon polymers that are poorly soluble in $scCO_2$ to CO_2-processable copolymers. iCVD copolymer thin films have demonstrated patterns with 300 nm feature size using CO_2 development, which is comparable with the resolution of CO_2 resists produced by spin-on technology. The combination of iCVD imaging materials with CO_2 development illustrates a complete solventless lithography process.

7.2 Future Directions

This thesis has opened the avenue for many opportunities in polymer vapor-phase synthesis. First, other initiator chemistry can be explored. Free radical UV initiators, for example, can be introduced to substitute thermal initiators and eliminate the use of filaments. Cationic and anionic initiators could be utilized to synthesize vinyl monomers that are difficult to polymerize via free radical mechanism. Second, it would be interesting to investigate other polymerization chemistry, such as vapor-phase graft polymerization, which can retain bulk properties of substrates while providing defined surface chemistry. Furthermore, chemical bonding created between the substrates and synthesized thin films can promote film stability and adhesion. Research in this direction will certainly increase the toolset that we can utilize to further understand the mechanism of vapor phase synthesis and to broaden application of polymer thin films.

From the perspective of applications, a wide variety of functional polymer coatings can be synthesized from their vinyl monomers, for example, coatings for controlled drug release,[1] coatings to promote or inhibit cell adhesion/proliferation,[2] hydrophilic/hydrophobic coatings, etc. This vapor phase synthesis method also has the capability to create copolymers that are

difficult to synthesize using solution approaches due to monomer incompatibility or insolubility issues.

More importantly, the solvent-free nature of vapor phase synthesis technique enables coating polymers with desirable properties to substrates with a wide range of morphologies, such as non-planar surface, three-dimensional structures, nanofibers, and nanoparticles. Research in this direction will bring new opportunities in creating surface with peculiar properties and improving devices' performance.

7.3 References

(1) Dashevsky, A.; Kolter, K.; Bodmeier, R. *Int. J. Pharm.* **2004,** *279*, 19.

(2) Harkes, G.; Feijen, J.; Dankert, J. *Biomaterials* **1991,** *12*, 853.